

A LOW-ORDER LOCKING-FREE MULTISCALE FINITE ELEMENT METHOD FOR ISOTROPIC ELASTICITY*

ANTÔNIO TADEU A. GOMES[†], WESLEY S. PEREIRA[‡], AND FRÉDÉRIC VALENTIN[§]

Abstract. The multiscale hybrid-mixed (MHM) method consists of a multi-level strategy to approximate the solution of boundary value problems with heterogeneous coefficients. In this context, we propose a family of low-order finite elements for the linear elasticity problem which are free from Poisson locking. The finite elements rely on face degrees of freedom associated with multiscale bases obtained from local Neumann problems with piecewise polynomial interpolations on faces. We establish sufficient refinement levels on the fine-scale mesh such that the MHM method is well-posed, optimally convergent under local regularity conditions, and locking-free. Two-dimensional numerical tests assess theoretical results.

Key words. multiscale finite element, domain decomposition, polytopes, elasticity, high performance computing, locking-free

AMS subject classifications. 65N30, 65N12, 65N22

1. Introduction. The Multiscale Hybrid-Mixed (MHM) methods are upscaling numerical strategies to solve boundary value problems on coarse partitions [1, 15]. As in other multiscale finite element methods, the MHM methods use localized multiscale basis functions to recover structures of the solution lost by the unresolved fine scales. From a computational viewpoint, this class of methods fit well in massively parallel computer systems because they allow for the multiscale basis functions to be computed in a decoupled fashion. The global degrees of freedom in the MHM methods localize on the faces of the mesh skeleton, and convergence can be achieved without refining the global partition [4, 12].

The MHM method was introduced to the two- and three-dimensional linear elasticity model in [13] using polynomial interpolations on faces and in the second-level discretization. This work was recently extended to global polytopal partitions and new finite elements [12], encompassing discontinuous interpolations on faces and refined local meshes. Both works use the continuous Galerkin method on top of the displacement elasticity formulation to build their multiscale basis functions. The MHM-Hdiv method [7] uses the same global problem from [13] but, in contrast, its local problems

*Submitted to the editors DATE.

Funding: This work was partially funded by the MCTI/RNP-Brazil under the HPC4E Project. The second author was partially supported by the CNPq/Brazil No. 140764/2015-1, by the company Bull Ltda and the SCAC from the French Embassy in Brazil under the CIFRE program. The third author was partially supported by CNPq/Brazil No. 301576/2013-0. This work was authored in part by the National Renewable Energy Laboratory, operated by Alliance for Sustainable Energy, LLC, for the U.S. Department of Energy (DOE) under Contract No. DE-AC36-08GO28308. The views expressed in the presentation do not necessarily represent the views of the DOE or the U.S. Government. The U.S. Government retains and the publisher, by accepting the article for publication, acknowledges that the U.S. Government retains a nonexclusive, paid-up, irrevocable, worldwide license to publish or reproduce the published form of this work, or allow others to do so, for U.S. Government purposes.

[†]Department of Computational and Mathematical Methods, National Laboratory for Scientific Computing - LNCC, Av. Getúlio Vargas, 333, 25651-070 Petrópolis - RJ, Brazil (atagomes@lncc.br)

[‡]Computational Science Center, National Renewable Energy Laboratory - NREL, 15257 Denver West Parkway Golden, CO 80401 US (wesley.dasilvapereira@nrel.gov)

[§]Department of Computational and Mathematical Methods, National Laboratory for Scientific Computing - LNCC, Av. Getúlio Vargas, 333, 25651-070 Petrópolis - RJ, Brazil and Nachos Project-Team, Inria Sophia Antipolis - Méditerranée, 2004 Route des Lucioles, 06902 Valbonne, France (valentin@lncc.br, frederic.valentin@inria.fr)

use mixed finite elements to recover a global Hdiv-conforming numerical stress tensor. The MHM method proposed in [18] uses the same interpolation spaces from [12] but a different local-level solver that deals with quasi-incompressible isotropic materials. This last work lacks proper stability and convergence analyses, and the locking-free property validation. We shall highlight that all four examples use the same global level problem and the choice of local level solver depend on the problem one wants to solve.

Inf-sup stability of most of the MHM methods presented in the literature relies on high-order polynomial spaces in the local level, e.g., [1, 2, 8, 11, 13, 14, 17]. A new way to prove stability was introduced in [4] for the two-dimensional Poisson equation. It encompasses the low-order global-local pairs (ℓ, ℓ) and $(\ell, \ell + 1)$, where ℓ is the polynomial degree used in the first-level solver. Low order finite elements are appealing for multiscale problems since they are computationally cheaper option for low-regularity problems.

It is well-known that standard low-order finite element methods applied to the displacement formulation of nearly incompressible elasticity problems result in poor observed convergence rates [3]. In the h -version of the continuous Galerkin method using piecewise linear polynomials on triangular meshes, the theoretical convergence rate only hold for h sufficiently small. This phenomenon is commonly known as locking (or Poisson locking). One way to circumvent this issue is to rewrite the elasticity problem in its mixed version, and approximate stress and displacement fields separately. Another possibility is to introduce an extra pressure variable, mimicking what is done in the Stokes problem. Since the choice of pairs of inf-sup stable approximation spaces is non-trivial in both cases, a classical approach to overcome this limitation employs stabilized schemes [10].

In this paper, we provide the stability and a priori convergence analysis for the family of finite elements proposed in [18]. The stability of the MHM method is based on the low-order global-local compromises (ℓ, ℓ) and $(\ell, \ell + 1)$ following closely [4]. We prove optimal mesh-based convergence for displacement, pressure and traction approximations under local regularity assumptions. We show the resulting MHM method is locking-free in the sense that the stability and a convergence constants do not degenerate when the Poisson ratio approaches $1/2$. The second-level solver uses a Least Squares stabilization for the Galerkin method [10], which possibly adopting the (appealing) equal-order polynomial spaces for displacement and pressure. We present some analytical numerical tests to verify the theoretical properties. We find an additional $O(+H/2)$ convergence in the skeleton-based refinement strategy, that was also observed in other families of MHM methods, e.g., [12, 4].

Using a problem with nearly incompressible materials, we verify the MHM method from [12, 18] improves the robustness of the continuous Galerkin method using compatible configurations between them. The same example shows how the locking-free finite elements present here and the Galerkin Least Squares method from [10] solves the Poisson locking issue. Finally, we test the versatility of the MHM method to solve a heterogeneous elasticity problem in a composite domain with nearly incompressible materials. We show it is sufficient to use the locking-free finite elements only in the nearly incompressible region to improve overall accuracy of the MHM solver.

The paper's outline is as follows. In [section 2](#), we present the isotropic elasticity problem in its classical and displacement-pressure forms. In [section 3](#), we revisit the MHM method from [12] that handles high-contrast heterogeneous coefficients using a multi-level approach. In [section 4](#), we present a family of stabilized MHM methods based on the Least-Squares stabilization of the Galerkin method. We prove the those

methods are well-posed and locking-free. As a subproduct, we show how to adapt the original Galerkin Least Squares method to pure Neumann problems. We prove the family of methods is optimally convergent under local regularity conditions in [section 5](#). We dedicate [section 6](#) to the numerical validation of the theory, and to show some numerical estimates of the MHM method. We present some concluding remarks in [section 7](#).

Remark 1.1. Above, and hereafter, we adopt the typical function spaces and differential operators [9]. The **bold** style indicates d -dimensional vector spaces, e.g., $\mathbf{L}^2(\Omega) := L^2(\Omega)^d$.

2. The elasticity problem. Let $\Omega \subset \mathbb{R}^d$, $d \in \{2, 3\}$, be an open and bounded domain with polygonal Lipschitz boundary $\partial\Omega = \overline{\Gamma_D} \cup \overline{\Gamma_N}$, $\Gamma_D \cap \Gamma_N = \emptyset$, and $\Gamma_D \neq \emptyset$. Consider the elasticity problem of finding a displacement $\mathbf{u} : \Omega \rightarrow \mathbb{R}^d$ that satisfies

$$(2.1) \quad -\nabla \cdot (\underline{\boldsymbol{\sigma}}(\mathbf{u})) = \mathbf{f} \text{ in } \Omega, \quad \mathbf{u} = \mathbf{0} \text{ on } \Gamma_D \text{ and } \underline{\boldsymbol{\sigma}}(\mathbf{u}) \mathbf{n} = \mathbf{g} \text{ on } \Gamma_N,$$

where $\mathbf{f} \in \mathbf{L}^2(\Omega)$ is the distributed load, $\mathbf{g} \in \mathbf{L}^2(\Gamma_N)$ is the traction, \mathbf{n} is the outward unit normal vector field defined a.e. on $\partial\Omega$, $\boldsymbol{\sigma} := \underline{\boldsymbol{\sigma}}(\mathbf{u})$ is the isotropic stress tensor

$$(2.2) \quad \underline{\boldsymbol{\sigma}}(\mathbf{u}) := 2G \left(\underline{\boldsymbol{\varepsilon}}(\mathbf{u}) + \frac{\nu}{1-2\nu} (\nabla \cdot \mathbf{u}) I_d \right),$$

$G, \nu \in L^\infty(\Omega)$ are the shear modulus and the Poisson's ratio, that possibly depend on Ω , $I_d \in \mathbb{R}^{d \times d}$ is the identity matrix, and $\underline{\boldsymbol{\varepsilon}}(\mathbf{u}) := (\nabla \mathbf{u} + (\nabla \mathbf{u})^t)/2$ is the infinitesimal strain tensor. We assume there exist $G_0, \nu_0 \in \mathbb{R}$ such that $0 < G_0 \leq G$ and $0 < \nu_0 \leq \nu < 1/2$ a.e. in Ω . Under these assumptions, there exists a unique solution $\mathbf{u} \in \mathbf{H}^1(\Omega)$ for (2.1) in a distributional sense via the BNB Theorem (c.f. [9, Theorem 2.6]).

Materials with high Poisson's ratio ($\nu \approx 1/2$) are usually referred as nearly incompressible, or quasi-incompressible. We call *Poisson locking phenomenon* the poor convergence order appearing in a numerical method when used to obtain approximate solutions to linear elasticity problems with nearly incompressible materials. This phenomenon occurs, for instance, in low-order continuous Galerkin formulations for (2.1) using piecewise polynomials on triangular and quadrilateral meshes [3].

A well known technique to avoid the Poisson locking starts by rewriting (2.1) in an equivalent mixed problem that approximates stress and displacement fields separately. Alternatively, consider the following displacement-pressure mixed form proposed in [16]

$$(2.3) \quad \begin{aligned} -\nabla \cdot (2G \underline{\boldsymbol{\varepsilon}}(\mathbf{u})) + \nabla \cdot (p I_d) &= \mathbf{f} & \text{in } \Omega, \\ \nabla \cdot \mathbf{u} + \epsilon p &= 0 & \text{in } \Omega, \\ \mathbf{u} &= \mathbf{0} & \text{on } \Gamma_D, \\ (2G \underline{\boldsymbol{\varepsilon}}(\mathbf{u}) - p I_d) \mathbf{n} &= \mathbf{g} & \text{on } \Gamma_N, \end{aligned}$$

where p is the (Herrmann) pressure

$$(2.4) \quad p := -\frac{1}{\epsilon} \nabla \cdot \mathbf{u}, \quad \text{and} \quad \epsilon := \frac{1-2\nu}{2G\nu}.$$

From a practical viewpoint, however, obtaining inf-sup stable numerical methods for usual discrete mixed formulations is non-trivial [5, §8.12.1]. A classical approach to

overcome the inf-sup limitation of (2.3) that keeps the desirable locking-free property is to employ stabilized schemes [10]. Subsection 4.2 presents the Galerkin Least Squares (GaLS) method, a stabilized finite element scheme to solve displacement-pressure mixed formulation.

3. The MHM method. Let \mathcal{P} be a collection of open and bounded d -polytopes K , such that $\overline{\Omega} = \cup_{K \in \mathcal{P}} \overline{K}$. Associated to $K \in \mathcal{P}$, we define the spaces

$$\begin{aligned} \mathbf{V}_{\text{rm}}(K) &:= \left\{ \mathbf{v}^{\text{rm}} \in \mathbf{H}^1(K) : \underline{\boldsymbol{\varepsilon}}(\mathbf{v}^{\text{rm}}) = 0 \right\}, \\ \tilde{\mathbf{V}}(K) &:= \left\{ \tilde{\mathbf{v}} \in \mathbf{H}^1(K) : \int_K \tilde{\mathbf{v}} \cdot \mathbf{v}^{\text{rm}} \, dx = 0, \quad \forall \mathbf{v}^{\text{rm}} \in \mathbf{V}_{\text{rm}}(K) \right\}, \end{aligned}$$

The functions $\mathbf{v}^{\text{rm}} \in \mathbf{V}_{\text{rm}}(K)$, known as rigid body motions, can be written as $\mathbf{v}^{\text{rm}}(\mathbf{x}) = \mathbf{a} + \beta(-x_2, x_1)$, if $d = 2$, and $\mathbf{v}^{\text{rm}}(\mathbf{x}) = \mathbf{a} + \mathbf{b} \times \mathbf{x}$, if $d = 3$, where $\mathbf{a}, \mathbf{b} \in \mathbb{R}^d$ and $\beta \in \mathbb{R}$. Therefore, $\mathbf{V}_{\text{rm}}(K)$ is a finite dimensional space of dimension $d(d+1)/2$. We also define the global spaces associated to \mathcal{P}

$$\begin{aligned} \mathbf{\Lambda} &:= \left\{ \boldsymbol{\tau} \mathbf{n}^K|_{\partial K}, \quad \forall K \in \mathcal{P} : \boldsymbol{\tau} \in H(\mathbf{div}; \Omega), \quad \boldsymbol{\tau} \mathbf{n}|_{\Gamma_N} = \mathbf{0} \right\}, \\ \mathbf{V}_{\text{rm}} &:= \left\{ \mathbf{v}^{\text{rm}} \in \mathbf{L}^2(\Omega) : \mathbf{v}^{\text{rm}}|_K \in \mathbf{V}_{\text{rm}}(K), \quad \forall K \in \mathcal{P} \right\}, \\ \tilde{\mathbf{V}} &:= \left\{ \tilde{\mathbf{v}} \in \mathbf{L}^2(\Omega) : \tilde{\mathbf{v}}|_K \in \tilde{\mathbf{V}}(K), \quad \forall K \in \mathcal{P} \right\}, \end{aligned}$$

where the symbol \mathbf{n}^K denotes the outward unit normal vector field on the boundary ∂K . Note the functions $\boldsymbol{\mu} \in \mathbf{\Lambda}$ belong to $\mathbf{H}^{-\frac{1}{2}}(\partial K)$ for each $K \in \mathcal{P}$.

We denote by Π_{RM} the $\mathbf{L}^2(\Omega)$ projection onto \mathbf{V}_{rm} , i.e., given $\mathbf{v} \in \mathbf{H}^1(\mathcal{P}) := \tilde{\mathbf{V}} \oplus \mathbf{V}_{\text{rm}}$, the function $\Pi_{RM} \mathbf{v}|_K$ satisfies

$$(3.1) \quad \int_K \Pi_{RM} \mathbf{v} \cdot \mathbf{v}^{\text{rm}} \, dx = \int_K \mathbf{v} \cdot \mathbf{v}^{\text{rm}} \, dx \quad \text{for all } \mathbf{v}^{\text{rm}} \in \mathbf{V}_{\text{rm}}(K),$$

which immediately leads to the following estimates for all $\mathbf{v} \in \mathbf{H}^1(\mathcal{P})$

$$(3.2) \quad \|\mathbf{v} - \Pi_{RM} \mathbf{v}\|_{0,\Omega} \leq \|\mathbf{v}\|_{0,\Omega} \quad \text{and} \quad \|\underline{\boldsymbol{\varepsilon}}(\mathbf{v} - \Pi_{RM} \mathbf{v})\|_{0,\mathcal{P}} \leq \|\underline{\boldsymbol{\varepsilon}}(\mathbf{v})\|_{0,\mathcal{P}}.$$

Hereafter, $\|\cdot\|_{m,D}$ and $|\cdot|_{m,K}$ denote the usual norm and semi-norm, respectively, in the spaces $H^m(D)$, $\mathbf{H}^m(D)$ and $H^m(D)^{d \times d}$, for $m \in \mathbb{N} \cap \{0\}$ and $D \subset \mathbb{R}^d$, and

$$\|\cdot\|_{m,\mathcal{P}} := \left(\sum_{K \in \mathcal{P}} \|\cdot\|_{m,K}^2 \right)^{\frac{1}{2}}, \quad |\cdot|_{m,\mathcal{P}} := \left(\sum_{K \in \mathcal{P}} |\cdot|_{m,K}^2 \right)^{\frac{1}{2}}.$$

are a norm and a semi-norm in $\mathbf{H}^1(\mathcal{P})$. Also, we equip $\mathbf{\Lambda}$ with the norm

$$(3.3) \quad \|\boldsymbol{\mu}\|_{\mathbf{\Lambda}} := \sup_{\mathbf{v} \in \mathbf{H}^1(\mathcal{P}) \setminus \{0\}} \frac{\sum_{K \in \mathcal{P}} \langle \boldsymbol{\mu}, \mathbf{v} \rangle_{\partial K}}{\|\mathbf{v}\|_{1,\mathcal{P}}} \quad \text{for every } \boldsymbol{\mu} \in \mathbf{\Lambda}.$$

The notation $\langle \cdot, \cdot \rangle_{\partial K}$ represents the duality pairing between $\mathbf{H}^{-\frac{1}{2}}(\partial K)$ and $\mathbf{H}^{\frac{1}{2}}(\partial K)$ in a way that if $\mathbf{v} \in \mathbf{H}^1(K)$ and $\boldsymbol{\mu} \in \mathbf{L}^2(\partial K)$ then $\langle \boldsymbol{\mu}, \mathbf{v} \rangle_{\partial K} = \int_{\partial K} \boldsymbol{\mu} \cdot \mathbf{v} \, ds$.

We now present the continuous formulation that is basis for the MHM methods.

Global-local formulation. Let $T : \mathbf{\Lambda} \rightarrow \tilde{\mathbf{V}}$ and $\hat{T} : \mathbf{L}^2(\Omega) \rightarrow \tilde{\mathbf{V}}$ be the linear operators such that, on each $K \in \mathcal{P}$, $T(\boldsymbol{\mu})|_K$ and $\hat{T}(\mathbf{q})|_K$ are the unique solutions in $\tilde{\mathbf{V}}(K)$ of

$$(3.4) \quad a_K(T(\boldsymbol{\mu}), \tilde{\mathbf{v}}) = \langle \boldsymbol{\mu}, \tilde{\mathbf{v}} \rangle_{\partial K} \quad \text{for all } \boldsymbol{\mu} \in \mathbf{\Lambda}, \tilde{\mathbf{v}} \in \tilde{\mathbf{V}}(K),$$

$$(3.5) \quad a_K(\hat{T}(\mathbf{q}), \tilde{\mathbf{v}}) = \int_K \mathbf{q} \cdot \tilde{\mathbf{v}} \, dx + \int_{\partial K \cap \Gamma_N} \mathbf{g} \cdot \tilde{\mathbf{v}} \, ds \quad \text{for all } \mathbf{q} \in \mathbf{L}^2(\Omega), \tilde{\mathbf{v}} \in \tilde{\mathbf{V}}(K),$$

respectively, where $\tilde{\mathbf{v}} \in \tilde{\mathbf{V}}(K)$ and

$$a_K(\mathbf{u}, \mathbf{v}) := \int_K \left(2G \underline{\boldsymbol{\varepsilon}}(\mathbf{u}) : \underline{\boldsymbol{\varepsilon}}(\mathbf{v}) + \frac{1}{\varepsilon} (\nabla \cdot \mathbf{u}) (\nabla \cdot \mathbf{v}) \right) dx \quad \text{for all } \mathbf{u}, \mathbf{v} \in \mathbf{H}^1(\mathcal{P}).$$

Owing to these definitions, we can rewrite the solution of (2.1) equivalently as

$$(3.6) \quad \mathbf{u} = \mathbf{u}^{\text{rm}} + T(\boldsymbol{\lambda}) + \hat{T}(\mathbf{f}),$$

where $(\boldsymbol{\lambda}, \mathbf{u}^{\text{rm}}) \in \mathbf{\Lambda} \times \mathbf{V}_{\text{rm}}$ solves the following mixed problem

$$(3.7) \quad \sum_{K \in \mathcal{P}} [\langle \boldsymbol{\mu}, T(\boldsymbol{\lambda}) \rangle_{\partial K} + \langle \boldsymbol{\mu}, \mathbf{u}^{\text{rm}} \rangle_{\partial K}] = - \sum_{K \in \mathcal{P}} \langle \boldsymbol{\mu}, \hat{T}(\mathbf{f}) \rangle_{\partial K} \quad \text{for all } \boldsymbol{\mu} \in \mathbf{\Lambda},$$

$$(3.8) \quad \sum_{K \in \mathcal{P}} \langle \boldsymbol{\lambda}, \mathbf{v}^{\text{rm}} \rangle_{\partial K} = - \int_{\Omega} \mathbf{f} \cdot \mathbf{v}^{\text{rm}} \, dx \quad \text{for all } \mathbf{v}^{\text{rm}} \in \mathbf{V}_{\text{rm}}.$$

The formulation (3.4)–(3.8) is known as global-local formulation and is equivalent to (2.1) in a distributional sense as proved in [12]. The hybridization variable $\boldsymbol{\lambda}$ represents the traction vector field along the skeleton of \mathcal{P} , i.e.,

$$(3.9) \quad \boldsymbol{\lambda} = \boldsymbol{\sigma} \mathbf{n}^K \quad \text{on } \partial K \setminus \Gamma_N \quad \text{for all } K \in \mathcal{P}.$$

The MHM method for linear elasticity relies on the discretization of (3.4)–(3.8).

MHM method's discrete formulation. Let $\mathbf{\Lambda}_H$ be a discrete subspace of $\mathbf{\Lambda}$, and T_h and \hat{T}_h be linear operators that approximate T and \hat{T} . The discrete version of (3.7)–(3.8) is to search for $(\boldsymbol{\lambda}_H, \mathbf{u}_H^{\text{rm}}) \in \mathbf{\Lambda}_H \times \mathbf{V}_{\text{rm}}$ such that

$$(3.10) \quad \sum_{K \in \mathcal{P}} [\langle \boldsymbol{\mu}_H, T_h(\boldsymbol{\lambda}_H) \rangle_{\partial K} + \langle \boldsymbol{\mu}_H, \mathbf{u}_H^{\text{rm}} \rangle_{\partial K}] = - \sum_{K \in \mathcal{P}} \langle \boldsymbol{\mu}_H, \hat{T}_h(\mathbf{f}) \rangle_{\partial K} \quad \text{for all } \boldsymbol{\mu}_H \in \mathbf{\Lambda}_H,$$

$$(3.11) \quad \sum_{K \in \mathcal{P}} \langle \boldsymbol{\lambda}_H, \mathbf{v}^{\text{rm}} \rangle_{\partial K} = - \int_{\Omega} \mathbf{f} \cdot \mathbf{v}^{\text{rm}} \, dx \quad \text{for all } \mathbf{v}^{\text{rm}} \in \mathbf{V}_{\text{rm}}.$$

The post-processed discrete displacement solution is

$$(3.12) \quad \mathbf{u}_{Hh} := \mathbf{u}_H^{\text{rm}} + T_h(\boldsymbol{\lambda}_H) + \hat{T}_h(\mathbf{f}).$$

and $\boldsymbol{\lambda}_H$ is the discrete traction that approximates $\boldsymbol{\sigma} \mathbf{n}^K$ on $\partial K \setminus \Gamma_N$ for all $K \in \mathcal{P}$. In the sequel, we define $\mathbf{\Lambda}_H$, T_h and \hat{T}_h so that (3.10)–(3.11) is well-posed and $(\boldsymbol{\lambda}_H, \mathbf{u}_H^{\text{rm}})$ approximates $(\boldsymbol{\lambda}, \mathbf{u}^{\text{rm}})$, the solution of (3.7)–(3.8).

Remark 3.1. Equations (3.4) and (3.5) are classical weak formulations for

$$-\nabla \cdot (\underline{\boldsymbol{\sigma}}(T(\boldsymbol{\mu}))) = R_{\boldsymbol{\mu}} \text{ in } K \quad \text{and} \quad \underline{\boldsymbol{\sigma}}(T(\boldsymbol{\mu})) \mathbf{n}^K = \boldsymbol{\mu} \text{ on } \partial K,$$

and

$$\begin{aligned} -\nabla \cdot (\underline{\boldsymbol{\sigma}}(\hat{T}(\mathbf{f}))) &= \Pi_{RM}(\mathbf{f}) \text{ in } K \quad \text{and} \quad \underline{\boldsymbol{\sigma}}(\hat{T}(\mathbf{f})) \mathbf{n}^K = \mathbf{g} \text{ on } \partial K \cap \Gamma_N, \\ \underline{\boldsymbol{\sigma}}(\hat{T}(\mathbf{f})) \mathbf{n}^K &= \mathbf{0} \text{ on } \partial K \setminus \Gamma_N, \end{aligned}$$

respectively, where $R_{\boldsymbol{\mu}}$ is the unique function in $\mathbf{V}_{\text{rm}}(K)$ satisfying $\int_K R_{\boldsymbol{\mu}} \cdot \mathbf{v}^{\text{rm}} dx = -\langle \boldsymbol{\mu}, \mathbf{v}^{\text{rm}} \rangle_{\partial K}$ for all $\mathbf{v}^{\text{rm}} \in \mathbf{V}_{\text{rm}}(K)$. These are pure traction elasticity problems similar to (2.1) with the additional condition $T(\boldsymbol{\mu})|_K, \hat{T}(\mathbf{q})|_K \in \tilde{\mathbf{V}}(K)$; therefore, they admit a global-local formulation if we repeat the procedure on a partition \mathcal{P}_K of K . Thus, one may use the MHM method to build multi-level algorithms.

Remark 3.2. Equation (3.11) states the local equilibrium of the elastic body since $\boldsymbol{\lambda}_H$ is the discrete traction field on ∂K .

Remark 3.3. The mappings T_h and \hat{T}_h can be defined quite generally. The choice depends on which unknown one wants to approximate accurately and impacts the robustness of the method. For instance, to ensure that the method yields a numerical stress tensor $\underline{\boldsymbol{\sigma}}(\mathbf{u}_{Hh}) \in H(\mathbf{div}; \Omega)$, one may use a stress mixed finite element method to approximate (3.4) and (3.5) [7]. The continuous Galerkin method with piecewise polynomials on triangular meshes was used in [12] to discretize (3.4) and (3.5) and obtain T_h and \hat{T}_h . The operators T_h and \hat{T}_h for this work are defined in subsection 4.2.

4. Locking-free finite elements for the MHM method. The MHM method uses a multi-level discretization starting from the first-level partition \mathcal{P} . In this work, we specify the partitions and spaces used in a two-level version of the method.

4.1. Preliminaries. Without loss of generality, we shall use hereafter the terminology employed for three-dimensional domains. Hereafter, $h_D := \sup_{x,y \in D} |x - y|$ is the diameter of an arbitrary bounded set $D \subset \mathbb{R}^n$, $n \in \mathbb{N}$. The radius of the largest inscribed ball in D reads ρ_D , and the shape regularity of D is denoted by $\sigma_D := h_D/\rho_D$.

Let \mathcal{E} be the set of the faces in \mathcal{P} , and $\{\mathcal{E}_H\}_{H>0}$ be a family of simplicial conformal partitions of \mathcal{E} . For each $K \in \mathcal{P}$, let $\{\mathcal{T}_h^K\}_{h>0}$ be a shape-regular family of local simplicial conformal partitions of K , and define $\mathcal{T}_h := \cup_{K \in \mathcal{P}} \mathcal{T}_h^K$ for each $h > 0$. Finally, we state the three characteristic sizes used recurrently hereafter:

$$(4.1) \quad \mathcal{H} := \max_{K \in \mathcal{P}} h_K, \quad H := \max_{F \in \mathcal{E}_H} h_F, \quad h := \max_{\tau \in \mathcal{T}_h} h_{\tau}.$$

See Figure 1 for an illustration. Note that \mathcal{P} and \mathcal{T}_h can be nonconformal, which brings versatility in the choice of both global and local partitions.

On each $K \in \mathcal{P}$, we define the discrete spaces

$$\begin{aligned} \mathbf{V}_h(K) &:= \{\mathbf{v}_h \in C^0(K)^d : \mathbf{v}_h|_{\tau} \in \mathbb{P}_k(\tau)^d, \quad \forall \tau \in \mathcal{T}_h^K\}, \\ \tilde{\mathbf{V}}_h(K) &:= \mathbf{V}_h(K) \cap \tilde{\mathbf{V}}(K), \\ Q_h(K) &:= \{q_h \in C^0(K) : q_h|_{\tau} \in \mathbb{P}_k(\tau), \quad \forall \tau \in \mathcal{T}_h^K\}, \\ \boldsymbol{\Lambda}_H(K) &:= \{\boldsymbol{\mu}_H \in \mathbf{L}^2(\partial K) : \boldsymbol{\mu}_H|_F \in \mathbb{P}_{\ell}(F), \quad \forall F \in \mathcal{E}_H^K\}. \end{aligned}$$

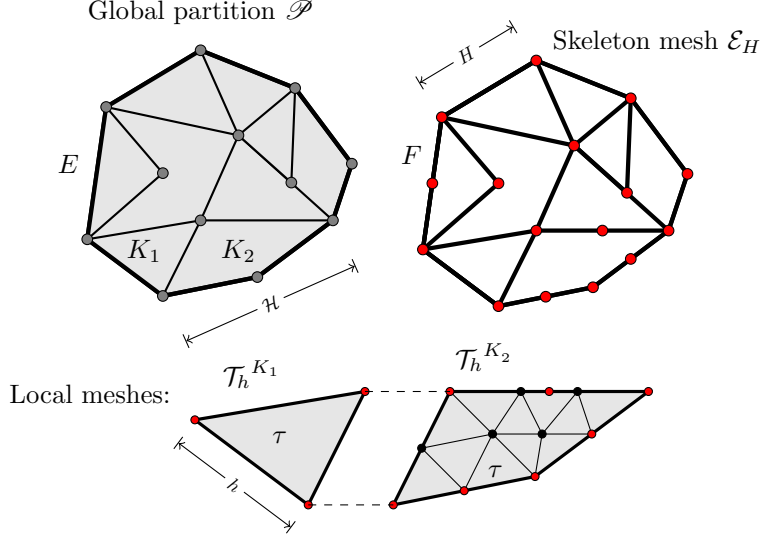


FIG. 1. A two-dimensional polygon partitioned by the meshes \mathcal{P} and \mathcal{T}_h . The fine-scale meshes, $\mathcal{T}_h^{K_1}$ and $\mathcal{T}_h^{K_2}$, are defined over $K_1, K_2 \in \mathcal{P}$, respectively. Elements K_1 and K_2 belong to \mathcal{P} ; faces E and F are in \mathcal{E} and \mathcal{E}_H , respectively; the simplexes τ belong to the affine mesh \mathcal{T}_h .

where $k, \ell \in \mathbb{N}^+$ and $\mathbb{P}_s(D)$ is the space of polynomials of degree less or equal to s on D . The corresponding global spaces are

$$\begin{aligned} \mathbf{V}_h &:= \{\mathbf{v}_h \in \mathbf{L}^2(\Omega) : \mathbf{v}_h|_K \in \mathbf{V}_h(K), \quad \forall K \in \mathcal{P}\}, \\ \tilde{\mathbf{V}}_h &:= \mathbf{V}_h \cap \tilde{\mathbf{V}}, \\ Q_h &:= \{q_h \in L^2(\Omega) : q_h|_K \in Q_h(K), \quad \forall K \in \mathcal{P}\}, \\ \mathbf{\Lambda}_H &:= \{\boldsymbol{\mu}_H \in \mathbf{\Lambda} : \boldsymbol{\mu}_H|_{\partial K} \in \mathbf{\Lambda}_H(K), \quad \forall K \in \mathcal{P}\}. \end{aligned}$$

The following sections use Poincaré and Korn's inequalities on $K \in \mathcal{P}$. It is well-known (see [9] for instance) that there exists a positive constant $C_{P,K}$ such that

$$(4.2) \quad \|\mathbf{v}\|_{0,K} \leq C_{P,K} h_K \|\mathbf{v}\|_{1,K} \quad \text{for all } \mathbf{v} \in \mathbf{H}^1(K) \cap \mathbf{L}_0^2(\Omega) \subset \tilde{\mathbf{V}}(K).$$

The Korn's inequality on the space $\tilde{\mathbf{V}}(K)$ was proved in [12], i.e., there exists a positive constant $C_{korn,K}$, independent of h_K , such that

$$(4.3) \quad \|\tilde{\mathbf{v}}\|_{1,K} \leq C_{korn,K} \|\underline{\boldsymbol{\varepsilon}}(\tilde{\mathbf{v}})\|_{0,K} \quad \text{for all } \tilde{\mathbf{v}} \in \tilde{\mathbf{V}}(K).$$

Finally, we use the following inverse inequality in the sequel

$$(4.4) \quad C_I \sum_{\tau \in \mathcal{T}_h^K} h_\tau^2 \left(\frac{1}{h_K^2} \|\underline{\boldsymbol{\varepsilon}}(\mathbf{v}_h)\|_{0,\tau}^2 + \|\nabla \cdot \underline{\boldsymbol{\varepsilon}}(\mathbf{v}_h)\|_{0,\tau}^2 \right) \leq \|\underline{\boldsymbol{\varepsilon}}(\mathbf{v}_h)\|_{0,K}^2,$$

for all $\mathbf{v}_h \in \mathbf{V}_h(K)$. The constant C_I depends only the polynomial order k and d using standard arguments, e.g., [9, Lemma 1.138]. Hereafter, we use C, C_1, C_2, \dots , for various positive constants which do not depend on H or h , and do not degenerate when the Poisson ratio approaches $1/2$.

Remark 4.1. For star-shaped elements, the constant $C_{P,K}$ in (4.2) depends only on d and the shape of K . See [23, 19, 24] for different works on this topic.

4.2. The Galerkin Least Squares formulation. Let $(T_h, T_h^p) : \mathbf{\Lambda} \rightarrow \tilde{\mathbf{V}}_h \times Q_h$ and $(\hat{T}_h, \hat{T}_h^p) : \mathbf{L}^2(\Omega) \rightarrow \tilde{\mathbf{V}}_h \times Q_h$ be linear operators defined by the following rule: for each $\boldsymbol{\mu} \in \mathbf{\Lambda}$, $\mathbf{q} \in \mathbf{L}^2(\Omega)$, $(T_h, T_h^p)(\boldsymbol{\mu})$ and $(\hat{T}_h, \hat{T}_h^p)(\mathbf{q})$ satisfy

$$(4.5) \quad B_K(T_h(\boldsymbol{\mu}), T_h^p(\boldsymbol{\mu}); \tilde{\mathbf{v}}_h, q_h) = \langle \boldsymbol{\mu}, \tilde{\mathbf{v}}_h \rangle_{\partial K},$$

$$(4.6) \quad B_K(\hat{T}_h(\mathbf{q}), \hat{T}_h^p(\mathbf{q}); \tilde{\mathbf{v}}_h, q_h) = F_K(\mathbf{q}; \tilde{\mathbf{v}}_h, q_h),$$

for all $(\tilde{\mathbf{v}}_h, q_h) \in \tilde{\mathbf{V}}_h(K) \times Q_h(K)$ and $K \in \mathcal{P}$, where

$$(4.7) \quad \begin{aligned} B_K(\mathbf{u}, p; \mathbf{v}, q) &:= \int_K (2G \underline{\boldsymbol{\varepsilon}}(\mathbf{u}) : \underline{\boldsymbol{\varepsilon}}(\mathbf{v}) - p(\nabla \cdot \mathbf{v}) - (\nabla \cdot \mathbf{u})q - \epsilon p q) dx \\ &- \alpha_K \sum_{\tau \in \mathcal{T}_h^K} h_\tau^2 \int_\tau (\nabla \cdot (2G \underline{\boldsymbol{\varepsilon}}(\mathbf{u}) - pI_d) \cdot \nabla \cdot (2G \underline{\boldsymbol{\varepsilon}}(\mathbf{v}) - qI_d)) dx, \end{aligned}$$

$$(4.8) \quad \begin{aligned} F_K(\mathbf{q}; \mathbf{v}, q) &:= \int_K \mathbf{q} \cdot \mathbf{v} dx + \int_{\partial K \cap \Gamma_N} \mathbf{g} \cdot \mathbf{v} ds \\ &+ \alpha_K \sum_{\tau \in \mathcal{T}_h^K} h_\tau^2 \int_\tau (\mathbf{q} \cdot \nabla \cdot (2G \underline{\boldsymbol{\varepsilon}}(\mathbf{v}) - qI_d)) dx. \end{aligned}$$

We choose the stabilization parameters α_K in the interval

$$(4.9) \quad 0 < \alpha_K < \frac{G_{0,K}}{2 \|G\|_{1,\infty,\mathcal{T}_h^K}^2} C_I,$$

where $G_{0,K} := \text{ess inf}_{\mathbf{x} \in K} G(\mathbf{x})$, and

$$(4.10) \quad \|G\|_{1,\infty,\mathcal{T}_h^K} := \max_{\tau \in \mathcal{T}_h^K} \sqrt{\|G\|_{L^\infty(\tau)}^2 + h_K^2 \|\nabla G\|_{L^\infty(\tau)}^2},$$

Notice that the Least Squares terms in (4.7) and (4.8) naturally induces the additional regularity over G , i.e., $G \in W^{1,\infty}(\mathcal{T}_h) := \{v \in L^\infty(\Omega) : v|_\tau \in W^{1,\infty}(\tau), \forall \tau \in \mathcal{T}_h\}$.

The operators (4.7)-(4.8) are inspired in the Galerkin Least Squares (GaLS) method from [10]. The former work was proposed for elasticity problems with constant coefficients G and ν , and mixed Dirichlet-Neumann boundary. Since the local problems (3.4)-(3.5) have pure Neumann boundary and heterogeneous elastic properties, we dedicate subsection 4.3 to adapt some results from [10].

Summary. The MHM method with finite elements based on the GaLS formulation reads as follows: Find the solution $(\boldsymbol{\lambda}_H, \mathbf{u}_H^{\text{rm}}) \in \mathbf{\Lambda}_H \times \mathbf{V}_{\text{rm}}$ of (3.10)-(3.11), such that (T_h, T_h^p) and (\hat{T}_h, \hat{T}_h^p) satisfy (4.5) and (4.8). This method provides the approximation for \mathbf{u} and $\boldsymbol{\sigma} \mathbf{n}^K|_{\partial K}$, equations (3.9) and (3.12), and for p and $\boldsymbol{\sigma}$ as follows

$$(4.11) \quad p_{Hh} := T_h^p(\boldsymbol{\lambda}_H) + \hat{T}_h^p(\mathbf{f}), \quad \boldsymbol{\sigma}_{Hh} := 2G \underline{\boldsymbol{\varepsilon}}(\mathbf{u}_{Hh}) - p_{Hh} I_d.$$

Remark 4.2. We can use $\tilde{\mathbf{v}}_h = \mathbf{0}$ and $q_h = 1$ in (4.5) and (4.6) to conclude the solution pair $(\mathbf{u}_{Hh}, p_{Hh})$ satisfies the following local compressibility constraint

$$(4.12) \quad \int_K (\nabla \cdot \mathbf{u}_{Hh} + \epsilon p_{Hh}) dx = 0 \quad \text{for every } K \in \mathcal{P}.$$

4.3. Well-posedness of the local formulation. The following results adapts the proofs in [10] to pure Neumann elasticity problems with heterogeneous coefficients G and ν . Also, we introduce the ϵ -norm in $L^2(K)$ as

$$(4.13) \quad \|q\|_{\epsilon,K} := \left(\int_K (1 + \epsilon) q^2 dx \right)^{\frac{1}{2}}, \quad \forall q \in L^2(K),$$

and the h -seminorm in $H^1(\mathcal{T}_h^K) := \{v \in L^2(K) : v|_{\tau} \in H^1(\tau), \forall \tau \in \mathcal{T}_h^K\}$ as

$$(4.14) \quad |q|_{h,K} := \left(\sum_{\tau \in \mathcal{T}_h^K} h_{\tau}^2 \|\nabla q\|_{0,\tau}^2 \right)^{\frac{1}{2}}, \quad \forall q \in H^1(\mathcal{T}_h^K).$$

We suppress using the sub-index h to shorten formulas inside the proofs.

The next result addresses the continuity of B_K (4.6) in $\tilde{\mathbf{V}}_h(K) \times Q_h(K)$.

LEMMA 4.3 (Boundness of B_K). *There is a positive constant C such that, for all $(\mathbf{u}_h, p_h), (\mathbf{v}_h, q_h) \in \tilde{\mathbf{V}}_h(K) \times Q_h(K)$, it holds*

$$(4.15) \quad B_K(\mathbf{u}_h, p_h; \mathbf{v}_h, q_h) \leq C (\|\underline{\boldsymbol{\varepsilon}}(\mathbf{u}_h)\|_{0,K}^2 + \|p_h\|_{\epsilon,K}^2)^{\frac{1}{2}} (\|\underline{\boldsymbol{\varepsilon}}(\mathbf{v}_h)\|_{0,K}^2 + \|q_h\|_{\epsilon,K}^2)^{\frac{1}{2}}.$$

Proof. We begin applying Cauchy-Schwarz inequalities in (4.7) to obtain

$$B_K(\mathbf{u}_h, p_h; \mathbf{v}_h, q_h) \leq N_K(\mathbf{u}_h, p_h) N_K(\mathbf{v}_h, q_h),$$

for $(\mathbf{u}_h, p_h), (\mathbf{v}_h, q_h) \in \tilde{\mathbf{V}}_h(K) \times Q_h(K)$, where $N_K : \tilde{\mathbf{V}}_h(K) \times Q_h(K) \rightarrow \mathbb{R}$ satisfies

$$\begin{aligned} N_K(\mathbf{u}_h, p_h)^2 := & \|2G\|_{L^\infty(K)} \|\underline{\boldsymbol{\varepsilon}}(\mathbf{u}_h)\|_{0,K}^2 + \|p_h\|_{0,K}^2 + \|\sqrt{\epsilon} p_h\|_{0,K}^2 + \|\nabla \cdot \mathbf{u}_h\|_{0,K}^2 \\ & + \alpha_K \sum_{\tau \in \mathcal{T}_h^K} h_{\tau}^2 \|\nabla \cdot (2G \underline{\boldsymbol{\varepsilon}}(\mathbf{u}_h) - p_h I_d)\|_{0,\tau}^2. \end{aligned}$$

Using Lemma A.2, we obtain

$$N_K(\mathbf{u}_h, p_h)^2 \leq \left(\|2G\|_{L^\infty(K)} + d + 4G_{0,K} \right) \|\underline{\boldsymbol{\varepsilon}}(\mathbf{u}_h)\|_{0,K}^2 + \|p_h\|_{\epsilon,K}^2 + 4G_{0,K} C_{0,K} \|p_h\|_{0,K}^2$$

and the analogous expression for $N_K(\mathbf{v}_h, q_h)^2$, so that the main result follows. \square

Using Lemma A.3, we prove the stability of B_K .

LEMMA 4.4. *There is a positive constant C such that, for all $(\tilde{\mathbf{u}}_h, p_h) \in \tilde{\mathbf{V}}_h(K) \times Q_h(K)$, there exists a pair $(\tilde{\mathbf{v}}_h, q_h) \in \tilde{\mathbf{V}}_h(K) \times Q_h(K)$ satisfying*

$$(4.16) \quad \frac{B_K(\tilde{\mathbf{u}}_h, p_h; \tilde{\mathbf{v}}_h, q_h)}{(\|\underline{\boldsymbol{\varepsilon}}(\tilde{\mathbf{v}}_h)\|_{0,K}^2 + \|q_h\|_{\epsilon,K}^2)^{1/2}} \geq C (\|\underline{\boldsymbol{\varepsilon}}(\tilde{\mathbf{u}}_h)\|_{0,K}^2 + \|p_h\|_{\epsilon,K}^2)^{1/2}.$$

Proof. Let $\tilde{\mathbf{u}}_h \in \tilde{\mathbf{V}}_h(K)$ and $p_h \in Q_h(K)$. Notice that

$$\begin{aligned} B_K(\tilde{\mathbf{u}}_h, p_h; \tilde{\mathbf{u}}_h, -p_h) = & \int_K (2G |\underline{\boldsymbol{\varepsilon}}(\tilde{\mathbf{u}}_h)|^2 + \epsilon p_h^2) dx \\ & - \alpha_K \sum_{\tau \in \mathcal{T}_h^K} h_{\tau}^2 (\|\nabla \cdot (2G \underline{\boldsymbol{\varepsilon}}(\tilde{\mathbf{u}}_h))\|_{0,\tau}^2 - \|\nabla p_h\|_{0,\tau}^2). \end{aligned}$$

From [Lemma A.1](#), we obtain

$$\int_K 2G |\underline{\boldsymbol{\varepsilon}}(\tilde{\mathbf{u}}_h)|^2 dx - \alpha_K \sum_{\tau \in \mathcal{T}_h^K} h_\tau^2 \|\nabla \cdot (2G \underline{\boldsymbol{\varepsilon}}(\tilde{\mathbf{u}}_h))\|_{0,\tau}^2 \geq C_3 \|\underline{\boldsymbol{\varepsilon}}(\tilde{\mathbf{u}}_h)\|_{0,K}^2,$$

where $C_3 := (2G_{0,K} - \alpha_K C_I^{-1}) > 0$ using [\(4.9\)](#). Combine the two expressions above to obtain

$$(4.17) \quad B_K(\tilde{\mathbf{u}}_h, p_h; \tilde{\mathbf{u}}_h, -p_h) \geq C_3 \|\underline{\boldsymbol{\varepsilon}}(\tilde{\mathbf{u}}_h)\|_{0,K}^2 + \int_K \epsilon p_h^2 dx + \alpha_K |p_h|_{h,K}^2,$$

Next, let $\tilde{\mathbf{w}} \in \tilde{\mathbf{V}}_h(K)$ be a function for which the supremum of [Lemma A.3](#) holds and such that $\|\tilde{\mathbf{w}}\|_{1,K} = \|p_h\|_{0,K}$. Then, using the bilinearity of B_K , [Lemmas 4.3](#) and [A.3](#), and the Cauchy-Schwarz inequality, we get

$$\begin{aligned} B_K(\tilde{\mathbf{u}}_h, p_h; -\tilde{\mathbf{w}}, 0) &= B_K(\tilde{\mathbf{u}}_h, 0; -\tilde{\mathbf{w}}, 0) + B_K(0, p_h; -\tilde{\mathbf{w}}, 0) \\ &\geq -C_4 \|\underline{\boldsymbol{\varepsilon}}(\tilde{\mathbf{u}}_h)\|_{0,K} \|\tilde{\mathbf{w}}\|_{1,K} + \int_K p_h (\nabla \cdot \tilde{\mathbf{w}}) dx - \alpha_K \sum_{\tau \in \mathcal{T}_h^K} h_\tau^2 (\nabla \cdot (2G \underline{\boldsymbol{\varepsilon}}(\tilde{\mathbf{w}})), \nabla p_h)_\tau \\ &\geq -C_4 \|\underline{\boldsymbol{\varepsilon}}(\tilde{\mathbf{u}}_h)\|_{0,K} \|p_h\|_{0,K} + C_1 \|p_h\|_{0,K}^2 - C_2 |p_h|_{h,K} \|p_h\|_{0,K} \\ &\quad - \sqrt{\alpha_K} \left(\alpha_K \sum_{\tau \in \mathcal{T}_h^K} h_\tau^2 \|\nabla \cdot (2G \underline{\boldsymbol{\varepsilon}}(\tilde{\mathbf{w}}))\|_{0,\tau}^2 \right)^{1/2} \left(\sum_{\tau \in \mathcal{T}_h^K} h_\tau^2 \|\nabla p_h\|_{0,\tau}^2 \right)^{1/2}. \end{aligned}$$

Now we use [Lemma A.1](#), [\(4.9\)](#), $\|\tilde{\mathbf{w}}\|_{1,K} = \|p_h\|_{0,K}$ and the Cauchy-Schwarz inequality, to obtain

$$(4.18) \quad B_K(\tilde{\mathbf{u}}_h, p_h; -\tilde{\mathbf{w}}, 0) \geq -C_6 \|\underline{\boldsymbol{\varepsilon}}(\tilde{\mathbf{u}}_h)\|_{0,K}^2 + C_7 \int_K p_h^2 dx - C_8 |p_h|_{h,K}^2,$$

where $C_6 := \frac{C_4}{2\gamma_1}$, $C_6 := C_1 - \frac{C_4 \gamma_1}{2} - \frac{(C_2 + C_5)\gamma_2}{2}$ and $C_8 := \frac{C_2 + C_5}{2\gamma_2}$, and γ_1 and γ_2 are arbitrary positive constants.

Combining [\(4.17\)](#) and [\(4.18\)](#), we can define a constant C_9 such that

$$(4.19) \quad B_K(\tilde{\mathbf{u}}_h, p_h; \tilde{\mathbf{u}}_h - \delta \tilde{\mathbf{w}}, -p_h) \geq C_9 (\|\underline{\boldsymbol{\varepsilon}}(\tilde{\mathbf{u}}_h)\|_{0,K}^2 + \|p_h\|_{\epsilon,K}^2),$$

where $0 < \delta < \min \left\{ \frac{C_3}{C_6}, \frac{\alpha_K}{C_8} \right\}$. On the other hand, choosing $\delta^2 \leq \frac{1}{2}$, we obtain

$$(4.20) \quad \begin{aligned} \|\underline{\boldsymbol{\varepsilon}}(\tilde{\mathbf{u}}_h - \delta \tilde{\mathbf{w}})\|_{0,K}^2 + \|-p_h\|_{\epsilon,K}^2 &\leq 2\|\underline{\boldsymbol{\varepsilon}}(\tilde{\mathbf{u}}_h)\|_{0,K}^2 + 2\delta^2 \|\underline{\boldsymbol{\varepsilon}}(\tilde{\mathbf{w}})\|_{0,K}^2 + \|p_h\|_{\epsilon,K}^2 = \\ &= 2\|\underline{\boldsymbol{\varepsilon}}(\tilde{\mathbf{u}}_h)\|_{0,K}^2 + \int_K (1 + \epsilon + 2\delta^2) p_h^2 dx \leq 2(\|\underline{\boldsymbol{\varepsilon}}(\tilde{\mathbf{u}}_h)\|_{0,K}^2 + \|p_h\|_{\epsilon,K}^2), \end{aligned}$$

The main result follows from [\(4.19\)](#) and [\(4.20\)](#) using $\mathbf{v}_h = \tilde{\mathbf{u}}_h - \delta \tilde{\mathbf{w}}$, $q_h = -p_h$ and $C = C_9/\sqrt{2}$. \square

The boundness of F_K can be proved using the Cauchy-Schwarz and triangle inequalities, and [Lemma A.2](#). Therefore, [Lemmas 4.3](#) and [4.4](#) suffice to guarantee the well-posedness of the problems [\(4.5\)](#) and [\(4.6\)](#) using the Banach-Nečas-Babuška (BNB) Theorem [[9](#), Theorem 2.6]. As a direct result, the pairs (T_h, T_h^p) and (\hat{T}_h, \hat{T}_h^p)

are well-defined. Moreover, using Poincaré and Korn's inequalities (4.2)–(4.3), (4.19), (4.5), and (3.3), we obtain

$$\begin{aligned} \|T_h(\boldsymbol{\mu})\|_{1,\mathcal{D}}^2 + \|T_h^p(\boldsymbol{\mu})\|_{0,\Omega}^2 &\leq C \|\boldsymbol{\mu}\|_{\Lambda} \|T_h(\boldsymbol{\mu}) - \delta \tilde{\mathbf{w}}\|_{1,\mathcal{D}} \\ &\leq 2C \|\boldsymbol{\mu}\|_{\Lambda} \left(\|T_h(\boldsymbol{\mu})\|_{1,\mathcal{D}}^2 + \|T_h^p(\boldsymbol{\mu})\|_{0,\mathcal{D}}^2 \right)^{\frac{1}{2}}. \end{aligned}$$

choosing δ small enough. We proceed the same way for (4.6), together with a trace inequality, e.g., [20, Lemma 1.49], to conclude that there exists a positive constant C satisfying

$$(4.21) \quad \sqrt{\|T_h(\boldsymbol{\mu})\|_{1,\mathcal{D}}^2 + \|T_h^p(\boldsymbol{\mu})\|_{0,\Omega}^2} \leq C \|\boldsymbol{\mu}\|_{\Lambda}, \quad \forall \boldsymbol{\mu} \in \Lambda,$$

$$(4.22) \quad \sqrt{\|\hat{T}_h(\mathbf{q})\|_{1,\mathcal{D}}^2 + \|\hat{T}_h^p(\mathbf{q})\|_{0,\Omega}^2} \leq C (\|\mathbf{q}\|_{0,\Omega} + \|\mathbf{g}\|_{0,\Gamma_N}), \quad \forall \mathbf{q} \in \mathbf{L}^2(\Omega).$$

4.4. Well-Posedness of the MHM method. The well-posedness of the MHM method on polytopal partitions was previously discussed in [4, 12]. The main ingredient to achieve well-posedness is to prove T_h is injective on \mathcal{N}_H ,

$$(4.23) \quad \mathcal{N}_H := \left\{ \boldsymbol{\mu}_H \in \Lambda_H : \sum_{K \in \mathcal{D}} \langle \boldsymbol{\mu}_H, \mathbf{v}^{\text{rm}} \rangle_{\partial K} = 0, \quad \forall \mathbf{v}^{\text{rm}} \in \mathbf{V}_{\text{rm}} \right\}.$$

Since the local problems (4.5) are well-posed, T_h is injective on \mathcal{N}_H if and only if the following statement holds: (see the proof of [13, Lemma 6.1])

$$(4.24) \quad \boldsymbol{\mu}_H \in \mathcal{N}_H : \sum_{K \in \mathcal{D}} \langle \boldsymbol{\mu}_H, \tilde{\mathbf{v}}_h \rangle_{\partial K} = 0, \quad \forall \tilde{\mathbf{v}}_h \in \tilde{\mathbf{V}}_h \quad \Rightarrow \quad \boldsymbol{\mu}_H = \mathbf{0}.$$

Notice that, apart from $\tilde{\mathbf{V}}_h$, this condition has no relation with the local discrete scheme of the MHM method.

In [13], the authors prove the injectivity of T_h on two-dimensional problems using

1. $\mathcal{T}_h = \mathcal{D}$, and even polynomial degree ℓ under the constraint $k = \ell + 1$;
2. quadrilateral meshes $\mathcal{T}_h = \mathcal{D}$ under the constraint $k \geq \ell + 2$.

This result was extended in [12] for the case of two-level meshes \mathcal{T}_h that *match* \mathcal{E}_H , which means that each face f of an arbitrary $\tau \in \mathcal{T}_h$ is contained by at most a single $F \in \mathcal{E}_H$. Under the matching condition and assuming $k - d \geq \ell \geq 1$, there exists a Fortin operator $\Pi_h : \mathbf{H}^1(\mathcal{D}) \rightarrow \mathbf{V}_h$, i.e., an operator that satisfies

$$(4.25) \quad \begin{aligned} \int_F \Pi_h(\mathbf{v}) \cdot \boldsymbol{\mu}_H \, dx &= \int_F \mathbf{v} \cdot \boldsymbol{\mu}_H \, dx \quad \text{for all } \boldsymbol{\mu}_H \in \Lambda_H \quad \text{and } F \in \mathcal{E}_H, \\ \|\Pi_h(\mathbf{v})\|_{1,\mathcal{D}} &\leq C \|\mathbf{v}\|_{1,\mathcal{D}}, \end{aligned}$$

for all $\mathbf{v} \in \mathbf{H}^1(\mathcal{D})$. The existence of such a Fortin operator also guarantees the injectivity of T_h on \mathcal{N}_H [12, Theorem 4.4].

In the following result, we introduce a new sufficient condition for T_h to be injective on \mathcal{N}_H also based on the existence of a Fortin operator. We cover the cases $k = \ell + 1$ and $k = \ell$ for the two-dimensional case.

LEMMA 4.5. *Let $\Omega \subset \mathbb{R}^2$. Suppose \mathcal{T}_h matches \mathcal{E}_H , and one of the following conditions hold on each $K \in \mathcal{D}$:*

1. $k \geq \ell + 1 \geq 2$ and there is at least 1 node of \mathcal{T}_h^K on each edge $F \in \mathcal{E}_H \cap \partial K$;
2. $k \geq \ell \geq s$ and there is at least $(4 - s)$ nodes of \mathcal{T}_h^K on the interior of each edge $F \in \mathcal{E}_H \cap \partial K$, where $s \in \{1, 2, 3\}$.

There exists a mapping $\Pi_h : \mathbf{H}^1(\mathcal{P}) \rightarrow \mathbf{V}_h$ such that, for all $\mathbf{v} \in \mathbf{H}^1(\mathcal{P})$, (4.25) holds. As a consequence, T_h is injective on \mathcal{N}_H .

Proof. Define $\mathcal{X} = \{q \in H_0^1(0, 1) : q|_{(0,t)} \in \mathbb{P}_{k+1}(0, t) \text{ and } q|_{(t,1)} \in \mathbb{P}_{k+1}(t, 1)\}$, where $t \in (0, 1)$. Using the arguments in the proof of [4, Lemma 4], we conclude that all $\varphi \in \mathbb{P}_k(0, 1)$ satisfying $\int_0^1 \varphi q \, dx = 0$ for all $q \in \mathcal{X}$ are identically zero in $[0, 1]$. In the same sense, the arguments used to prove [4, Lemma 5] are still valid over partitions of $(0, 1)$ that are not equally spaced. This being noticed, define $\Pi_h(\mathbf{v})_i := \Pi_h^{BJPV}(v_i)$, for each $i = 1, \dots, d$, where $\Pi_h^{BJPV} : H^1(\mathcal{P}) \rightarrow C^0(\mathcal{P}) \cap \mathbb{P}_k(\mathcal{T}_h)$ is the operator from [4, Lemma 2]. Using the properties of Π_h^{BJPV} , we conclude Π_h satisfies the first equation in (4.25). Moreover, there exists a positive constant C_K such that

$$(4.26) \quad \|\Pi_h^{BJPV}(v)\|_{1,K} \leq C_K \|v\|_{1,K}, \quad \text{for all } v \in H^1(K),$$

for all $K \in \mathcal{P}$. Thus, we use (4.26) to complete the proof as follows

$$\|\Pi_h(\mathbf{v})\|_{1,\mathcal{P}}^2 = \sum_{K \in \mathcal{P}} \sum_{i=1}^d \|\Pi_h^{BJPV}(v_i)\|_{1,K}^2 \leq C \sum_{K \in \mathcal{P}} \sum_{i=1}^d \|v_i\|_{1,K}^2 \leq C \|\mathbf{v}\|_{1,\mathcal{P}}^2. \quad \square$$

For the three-dimensional case, one may use similar arguments to conclude that the Fortin mapping exists if, on each $K \in \mathcal{P}$,

1. $k = \ell = 1$ and there is at least three non-collinear nodes of \mathcal{T}_h^K on the interior of face $F \in \mathcal{E}_H \cap \partial K$;
2. $k = \ell + 1 = 2$ and there is at least one node of \mathcal{T}_h^K on the interior of each edge $E \subset \partial F$, where $F \in \mathcal{E}_H \cap \partial K$ is a face.

Provided T_h is injective, one may prove the well-posedness of the MHM method as follows.

THEOREM 4.6. *Suppose T_h is injective on \mathcal{N}_H . Then, there exist positive constants α_0 and β_0 , independent of H and h and that do not degenerate when the Poisson's ratio approaches $1/2$, such that*

$$(4.27) \quad \sum_{K \in \mathcal{P}} \langle \boldsymbol{\mu}_H, T_h(\boldsymbol{\mu}_H) \rangle_{\partial K} \geq \alpha_0 \|\boldsymbol{\mu}_H\|_{\Lambda}^2 \quad \text{for all } \boldsymbol{\mu}_H \in \mathcal{N}_H,$$

$$(4.28) \quad \sup_{\boldsymbol{\mu}_H \in \Lambda_H \setminus \{0\}} \frac{\sum_{K \in \mathcal{P}} \langle \boldsymbol{\mu}_H, \mathbf{v}^{\text{rm}} \rangle_{\partial K}}{\|\boldsymbol{\mu}_H\|_{\Lambda}} \geq \beta_0 \|\mathbf{v}^{\text{rm}}\|_{0,\Omega} \quad \text{for all } \mathbf{v}^{\text{rm}} \in \mathbf{V}_{\text{rm}}.$$

Then, (3.10)-(3.11) is well-posed.

Proof. We begin proving an auxiliary result. Let $\tilde{\mathbf{w}} \in \tilde{\mathbf{V}}_h$ be a function satisfying

Lemma A.3 and such that $\|\tilde{\mathbf{w}}\|_{1,K} = \|T_h^p(\boldsymbol{\mu})\|_{0,K}$. Therefore, for every $\delta > 0$,

$$\begin{aligned}
 & B_K(T_h(\boldsymbol{\mu}), T_h^p(\boldsymbol{\mu}); T_h(\boldsymbol{\mu}), 0) \\
 &= B_K\left(T_h(\boldsymbol{\mu}), T_h^p(\boldsymbol{\mu}); T_h(\boldsymbol{\mu}) - \frac{\delta}{2}\tilde{\mathbf{w}}, 0\right) + \frac{\delta}{2}B_K(T_h(\boldsymbol{\mu}), T_h^p(\boldsymbol{\mu}); \tilde{\mathbf{w}}, 0) \\
 &= B_K\left(T_h(\boldsymbol{\mu}), T_h^p(\boldsymbol{\mu}); T_h(\boldsymbol{\mu}) - \frac{\delta}{2}\tilde{\mathbf{w}}, -T_h^p(\boldsymbol{\mu})\right) + \frac{\delta}{2}B_K(-T_h(\boldsymbol{\mu}), -T_h^p(\boldsymbol{\mu}); -\tilde{\mathbf{w}}, 0) \\
 &\geq (C_3 - \delta C_6) \|\underline{\boldsymbol{\varepsilon}}(T_h(\boldsymbol{\mu}))\|_{0,K}^2 + \int_K (\epsilon + \delta C_7) |T_h^p(\boldsymbol{\mu})|^2 dx + \\
 &\quad + (\alpha_K - \delta C_8) \sum_{\tau \in \mathcal{T}_h^K} h_\tau^2 |T_h^p(\boldsymbol{\mu})|_{1,\tau}^2,
 \end{aligned}$$

where the positive constants C_3, C_6, C_7, C_8 are defined in the proof of **Lemma 4.4**. We can choose δ small enough to obtain a positive constant C such that

$$(4.29) \quad B_K(T_h(\boldsymbol{\mu}), T_h^p(\boldsymbol{\mu}); T_h(\boldsymbol{\mu}), 0) \geq C(\|\underline{\boldsymbol{\varepsilon}}(T_h(\boldsymbol{\mu}))\|_{0,K}^2 + \|T_h^p(\boldsymbol{\mu})\|_{0,K}^2),$$

for all $\boldsymbol{\mu} \in \boldsymbol{\Lambda}$ and $K \in \mathcal{P}$. We use this formula to prove (4.27).

Let $\boldsymbol{\mu}_H \in \mathcal{N}_H$ and, for every $\mathbf{v} \in \mathbf{H}^1(\mathcal{P})$, denote $\tilde{\mathbf{v}} = \mathbf{v} - \Pi_{RM}(\mathbf{v}) \in \tilde{\mathbf{V}}$. We can use (3.3), (4.23), (3.2), and $C_{korn} \geq 1$ to obtain

$$(4.30) \quad \|\boldsymbol{\mu}_H\|_{\boldsymbol{\Lambda}} \leq C_{korn} \sup_{\tilde{\mathbf{v}} \in \tilde{\mathbf{V}} \setminus \{\mathbf{0}\}} \frac{\sum_{K \in \mathcal{P}} \langle \boldsymbol{\mu}_H, \tilde{\mathbf{v}} \rangle_{\partial K}}{\|\tilde{\mathbf{v}}\|_{1,\mathcal{P}}} \leq C \sup_{\tilde{\mathbf{v}}_h \in \tilde{\mathbf{V}}_h \setminus \{\mathbf{0}\}} \frac{\sum_{K \in \mathcal{P}} \langle \boldsymbol{\mu}_H, \tilde{\mathbf{v}}_h \rangle_{\partial K}}{\|\tilde{\mathbf{v}}_h\|_{1,\mathcal{P}}}.$$

The constant C does not depend on h, H or \mathcal{H} (see, for instance, [13, Lemma 6.1] and [21, Lemma 10]). Equation (4.27) follows from (4.30), (4.5), **Lemma 4.3** and (4.29), in this order, with $q_h = \mathbf{0}$, and finally (4.5) once more. The inf-sup condition (4.28) follows directly from [12]. Equations (4.27) and (4.28) imply the stability and well-posedness of the formulation (3.10)-(3.11) using the classical saddle-point theory. \square

Remark 4.7. When there exists a Fortin operator $\Pi_h : \mathbf{H}^1(\mathcal{P}) \rightarrow \mathbf{V}_h$ satisfying (4.25), the constant C in (4.30) is bounded by C_{korn}, C_P and C from (4.25). The latter depends on the polynomial order k, d and $\sigma_{\mathcal{T}}$ for the case $k \geq \ell + 1$ as states [12, Lemma 4.2].

5. A priori error estimates for the MHM method. The convergence estimates can be split into two parts: local, related to T_h and \hat{T}_h inside each element $K \in \mathcal{P}$, and global, which is related to the best approximation of $\boldsymbol{\Lambda}$ in $\boldsymbol{\Lambda}_H$. The next result tackles the approximation properties of the local formulation, i.e., it shows how good (T_h, T_h^p) and (\hat{T}_h, \hat{T}_h^p) approximate $(T, -\epsilon^{-1} \nabla \cdot T)$ and $(\hat{T}, -\epsilon^{-1} \nabla \cdot \hat{T})$. Moreover, it states the discrete formulation is locking-free.

THEOREM 5.1. *Let $\boldsymbol{\mu} \in \boldsymbol{\Lambda}$ and $\mathbf{q} \in \mathbf{L}^2(\Omega)$ be such that $\tilde{\mathbf{u}} := T(\boldsymbol{\mu})|_K + \hat{T}(\mathbf{q})|_K \in \mathbf{H}^{s+1}(K)$ and $p := -\epsilon^{-1} \nabla \cdot \tilde{\mathbf{u}} \in H^s(K)$, with $1 \leq s \leq k$. The solutions $\tilde{\mathbf{u}}_h := T_h(\boldsymbol{\mu})|_K + \hat{T}_h(\mathbf{q})|_K$ and $p_h := T_h^p(\boldsymbol{\mu})|_K + \hat{T}_h^p(\mathbf{q})|_K$, defined using (4.5)-(4.6), satisfy the following estimate*

$$(5.1) \quad \|\tilde{\mathbf{u}} - \tilde{\mathbf{u}}_h\|_{1,K} + \|p - p_h\|_{0,K} \leq C h^s (|\tilde{\mathbf{u}}|_{s+1,K} + |p|_{s,K}).$$

Proof. Using the [Lemma 4.4](#), the consistency of the schemas (4.5)-(4.6) for $\tilde{\mathbf{u}} \in \mathbf{H}^2(K)$ and $\epsilon p \in H^1(K)$, and the proof of [Lemma 4.3](#), we obtain

$$\begin{aligned} & (\|\underline{\boldsymbol{\varepsilon}}(\tilde{\mathbf{u}}_h - \tilde{\mathbf{w}}_h)\|_{0,K}^2 + \|p_h - s_h\|_{\epsilon,K}^2)^{1/2} \leq C \left(\|2G\|_{L^\infty(K)} \|\underline{\boldsymbol{\varepsilon}}(\tilde{\mathbf{u}} - \tilde{\mathbf{w}}_h)\|_{0,K}^2 \right. \\ & \quad + \|p - s_h\|_{0,K}^2 + \|\sqrt{\epsilon}(p - s_h)\|_{0,K}^2 + \|\nabla \cdot (\tilde{\mathbf{u}} - \tilde{\mathbf{w}}_h)\|_{0,K}^2 \\ & \quad \left. + \alpha_K \sum_{\tau \in \mathcal{T}_h^K} h_\tau^2 \|\nabla \cdot (2G \underline{\boldsymbol{\varepsilon}}(\tilde{\mathbf{u}} - \tilde{\mathbf{w}}_h) - (p - s_h)I)\|_{0,\tau}^2 \right)^{\frac{1}{2}}, \end{aligned}$$

for all $(\tilde{\mathbf{w}}_h, s_h) \in \tilde{\mathbf{V}}(K) \times Q_h$. We then proceed like in the proof of [Lemmas A.1](#) and [A.2](#) and, using (4.14), obtain

$$(5.2) \quad \begin{aligned} & (\|\underline{\boldsymbol{\varepsilon}}(\tilde{\mathbf{u}}_h - \tilde{\mathbf{w}}_h)\|_{0,K}^2 + \|p_h - s_h\|_{\epsilon,K}^2)^{1/2} \leq C \left(\|\underline{\boldsymbol{\varepsilon}}(\tilde{\mathbf{u}} - \tilde{\mathbf{w}}_h)\|_{0,K}^2 \right. \\ & \quad \left. + \|p - s_h\|_{0,K}^2 + |p - s_h|_{h,K}^2 + \sum_{\tau \in \mathcal{T}_h^K} h_\tau^2 \|\nabla \cdot \underline{\boldsymbol{\varepsilon}}(\tilde{\mathbf{u}} - \tilde{\mathbf{w}}_h)\|_{0,\tau}^2 \right)^{\frac{1}{2}}, \end{aligned}$$

Now, we choose \mathbf{w}_h to be the Scott-Zhang interpolation [22] of $\tilde{\mathbf{u}}$ onto $\mathbf{V}_h(K)$ and define $\tilde{\mathbf{w}}_h := \mathbf{w}_h - \Pi_{RM} \mathbf{w}_h$. Therefore,

$$(5.3) \quad \|\underline{\boldsymbol{\varepsilon}}(\tilde{\mathbf{u}} - \tilde{\mathbf{w}}_h)\|_{0,K} \leq |\tilde{\mathbf{u}} - \mathbf{w}_h|_{1,K} \leq C h^s |\tilde{\mathbf{u}}|_{s+1,K},$$

$$(5.4) \quad \sum_{\tau \in \mathcal{T}_h^K} h_\tau^2 \|\nabla \cdot \underline{\boldsymbol{\varepsilon}}(\tilde{\mathbf{u}} - \tilde{\mathbf{w}}_h)\|_{0,\tau}^2 \leq d \sum_{\tau \in \mathcal{T}_h^K} h_\tau^2 |\tilde{\mathbf{u}} - \mathbf{w}_h|_{2,\tau}^2 \leq C h^{2s} |\tilde{\mathbf{u}}|_{s+1,K}^2.$$

Analogously, we use s_h as the Scott-Zhang interpolation of p onto $Q_h(K)$, and verify the existence of a positive constant C such that

$$(5.5) \quad \|p - s_h\|_{0,K} + |p - s_h|_{h,K} \leq C h^s |p|_{s,K}.$$

Now, we replace (5.3)-(5.5) into (5.2) to obtain

$$(5.6) \quad (\|\underline{\boldsymbol{\varepsilon}}(\tilde{\mathbf{u}}_h - \tilde{\mathbf{w}}_h)\|_{0,K}^2 + \|p_h - s_h\|_{\epsilon,K}^2)^{1/2} \leq C h^s \left(|\tilde{\mathbf{u}}|_{s+1,K}^2 + |p|_{s,K}^2 \right)^{\frac{1}{2}}.$$

Starting from the left side of (5.1) we use the Poincaré and Korn's inequalities (4.2) and (4.3), sum and subtract $\tilde{\mathbf{w}}_h$ and \tilde{s}_h , use the triangle inequality, and (5.3), (5.5), and (5.6), to complete the proof. \square

As for the global part of the method, we use the best approximation result in Λ_H from [12] to prove the following result.

THEOREM 5.2. *Suppose T_h is injective on \mathcal{N}_H , and that α_K satisfies (4.9) for all $K \in \mathcal{P}$. Moreover, suppose $\ell \geq 1$, and that there exists a mapping $\Pi_h : \mathbf{H}^1(\mathcal{P}) \rightarrow \mathbf{V}_h$ satisfying (4.25) for all $\mathbf{v} \in \mathbf{H}^1(\mathcal{P})$. Let \mathbf{u} be the solution of (2.1), and let $1 \leq s \leq k$ and $1 \leq m \leq \min\{s, \ell + 1\}$ be such that $\mathbf{u} \in \mathbf{H}^{s+1}(\mathcal{P})$, $p = -\epsilon^{-1} \nabla \cdot \tilde{\mathbf{u}} \in H^s(\mathcal{P})$ and $\boldsymbol{\sigma} \in H^m(\mathcal{P})^{d \times d}$. Then, there exists a positive constant C such that*

$$(5.7) \quad \begin{aligned} & \|\mathbf{u}^{\text{rm}} - \mathbf{u}_H^{\text{rm}}\|_{0,\Omega} + \|\boldsymbol{\lambda} - \boldsymbol{\lambda}_H\|_{\Lambda} \\ & \leq C \left(h^s (|\mathbf{u} - \mathbf{u}^{\text{rm}}|_{s+1,\mathcal{P}} + |p|_{s,\mathcal{P}}) + H^m |\boldsymbol{\sigma}|_{m,\mathcal{P}} \right). \end{aligned}$$

In addition, $\mathbf{u}_{Hh} := \mathbf{u}_H^{\text{rm}} + T_h(\boldsymbol{\lambda}_H) + \hat{T}_h(\mathbf{f})$, $p_{Hh} := T_h^p(\boldsymbol{\lambda}_H) + \hat{T}_h^p(\mathbf{f})$ and $\boldsymbol{\sigma}_{Hh} := 2G \underline{\boldsymbol{\varepsilon}}(\mathbf{u}_{Hh}) - p_{Hh} I_d$ satisfy

$$(5.8) \quad \begin{aligned} & \|\mathbf{u} - \mathbf{u}_{Hh}\|_{1,\mathcal{P}} + \|p - p_{Hh}\|_{0,\Omega} + \|\boldsymbol{\sigma} - \boldsymbol{\sigma}_{Hh}\|_{0,\Omega} \\ & \leq C \left(h^s (|\mathbf{u} - \mathbf{u}^{\text{rm}}|_{s+1,\mathcal{P}} + |p|_{s,\mathcal{P}}) + H^m |\boldsymbol{\sigma}|_{m,\mathcal{P}} \right). \end{aligned}$$

Proof. Equation (5.7) follows directly from the proof of the approximation result in [12], using Theorem 5.1 as the local error estimate. To prove (5.8), we decompose the error $\mathbf{u} - \mathbf{u}_{Hh}$ as follows

$$\begin{aligned} & \|\mathbf{u} - \mathbf{u}_{Hh}\|_{1,\mathcal{P}} \\ & \leq \|\mathbf{u}^{\text{rm}} - \mathbf{u}_{\mathcal{H}}^{\text{rm}}\|_{0,\Omega} + |\mathbf{u}^{\text{rm}} - \mathbf{u}_{\mathcal{H}}^{\text{rm}}|_{1,\mathcal{P}} + \|T(\boldsymbol{\lambda}) - T_h(\boldsymbol{\lambda}_H) + (\hat{T} - \hat{T}_h)(\mathbf{f})\|_{1,\mathcal{P}}. \end{aligned}$$

First, we use the triangular inequality, (4.21), (5.1) and (5.7) to obtain

$$\begin{aligned} & \|\mathbf{u}^{\text{rm}} - \mathbf{u}_{\mathcal{H}}^{\text{rm}}\|_{0,\Omega} + \|T_h(\boldsymbol{\lambda} - \boldsymbol{\lambda}_H) + (T - T_h)(\boldsymbol{\lambda}) + (\hat{T} - \hat{T}_h)(\mathbf{f})\|_{1,\mathcal{P}} \\ & \leq C (h^s (|\mathbf{u} - \mathbf{u}^{\text{rm}}|_{s+1,\mathcal{P}} + |p|_{s,\mathcal{P}}) + H^m |\boldsymbol{\sigma}|_{m,\mathcal{P}}). \end{aligned}$$

In [12], we proved there exists a constant C , depending only on Ω , the shape-regularity of \mathcal{P} , and the Poincaré and trace inequality constants, such that

$$|\mathbf{u}^{\text{rm}} - \mathbf{u}_{\mathcal{H}}^{\text{rm}}|_{1,\mathcal{P}} \leq C \left(\|\mathbf{u}^{\text{rm}} - \mathbf{u}_{\mathcal{H}}^{\text{rm}}\|_{0,\Omega} + |T(\boldsymbol{\lambda}) - T_h(\boldsymbol{\lambda}_H) + (\hat{T} - \hat{T}_h)(\mathbf{f})|_{1,\mathcal{P}} \right).$$

Thus, arguing as before, we conclude

$$|\mathbf{u}^{\text{rm}} - \mathbf{u}_{\mathcal{H}}^{\text{rm}}|_{1,\mathcal{P}} \leq C (h^s (|\mathbf{u} - \mathbf{u}^{\text{rm}}|_{s+1,\mathcal{P}} + |p|_{s,\mathcal{P}}) + H^m |\boldsymbol{\sigma}|_{m,\mathcal{P}}).$$

We collect the four last expressions to conclude the first part of (5.8). To estimate $\|p - p_{Hh}\|_{0,\Omega}$, we use Theorem 5.1 and sum up the contributions on each $K \in \mathcal{P}$. To estimate $\|\boldsymbol{\sigma} - \boldsymbol{\sigma}_{Hh}\|_{0,\Omega}$, observe that

$$\|\boldsymbol{\sigma} - \boldsymbol{\sigma}_{Hh}\|_{0,\Omega} \leq 2G (|\mathbf{u} - \mathbf{u}_{Hh}|_{1,\mathcal{P}} + \|p - p_{Hh}\|_{0,\Omega}).$$

The result follows from the previous estimates, and the proof is complete. \square

Remark 5.3. The constant C in (5.1) depends on $\text{ess inf}_{\mathbf{x} \in K} \nu_0(\mathbf{x}) \geq \nu_0$. Since the locking behavior appears for high values of ν_0 , i.e., $\nu_0 \approx 1/2$, this does not change the conclusion that the presented local method is free of locking. Moreover, if the material property ϵ is constant on each $K \in \mathcal{P}$, one may eliminate this dependency following the proof of [10, Theorem 3.1]. Since ϵ does not appear explicitly in the global problem (3.10)-(3.11), and the stability and convergence constants for the formulations (4.5) and (4.6) do not degenerate when $\epsilon \rightarrow 0$, the MHM method is locking-free.

Remark 5.4. Theorem 5.2 states the MHM method's $(H + h)$ -convergence, and that means we improve accuracy by refining the face and local partitions \mathcal{E}_H and \mathcal{T}_h . In order to achieve the typical \mathcal{H} -convergence, one must define a family of global partitions $\{\mathcal{P}_{\mathcal{H}}\}_{\mathcal{H}>0}$ of Ω such that all constants involved in the analysis stays bounded when $\mathcal{H} \rightarrow 0$. We refer to [12] for a detailed discussion on this topic.

Remark 5.5. Under local smoothing conditions, one may improve the \mathbf{L}^2 -convergence order of the displacement error in Theorem 5.1, adapting the procedure from the proof of [10, Theorem 3.1]. To improve global \mathbf{L}^2 -convergence order in Theorem 5.2, we proceed exactly as in [12].

6. Numerical Results. This section assesses the MHM method numerically on nearly incompressible materials. We use the following two-dimensional model problem proposed in [6]. Let $\Omega := [0, 1]^2$ be an isotropic elastic domain with shear modulus $G = 1$, Poisson's ratio $\nu \in \{0.2, 0.3, 0.4, 0.49, 0.499, 0.4999, 0.49999\}$, and let

$$\mathbf{u} = \{u_1, u_2\},$$

$$\begin{aligned} u_1(x, y) &= (\cos(2\pi x) - 1) \sin(2\pi y) + \frac{1 - 2\nu}{2} \sin(\pi x) \sin(\pi y), \\ u_2(x, y) &= (1 - \cos(2\pi y)) \sin(2\pi x) + \frac{1 - 2\nu}{2} \sin(\pi x) \sin(\pi y), \end{aligned}$$

be the exact solution of (2.1) with $\Gamma_D = \partial\Omega$. The pressure is $p := -\frac{2G\nu}{1-2\nu} \nabla \cdot \mathbf{u} = -2\pi\nu \sin(\pi(x+y))$, $\boldsymbol{\sigma} := \underline{\boldsymbol{\sigma}}(\mathbf{u})$, and $\mathbf{f} = \{f_1, f_2\}$ is defined as follows

$$\begin{aligned} f_1(x, y) &= \pi^2 (4 \sin(2\pi y)(2 \cos(2\pi x) - 1) - \cos(\pi(x+y)) + (1 - 2\nu) \sin(\pi x) \sin(\pi y)), \\ f_2(x, y) &= \pi^2 (4 \sin(2\pi x)(1 - 2 \cos(2\pi y)) - \cos(\pi(x+y)) + (1 - 2\nu) \sin(\pi x) \sin(\pi y)). \end{aligned}$$

In the following, we verify the theoretical results and show some numerical estimates. The underlying algorithm and the implementation aspects of the MHM method implemented for the test cases were presented in [12].

6.1. The Poisson locking phenomenon. In this section, we see how high Poisson's ratios influence the precision of the MHM-Ga, MHM-GaLS, stdGalerkin, and GaLS methods. We use structured triangular partitions in every stage of all methods, and the MHM methods use trivial skeleton meshes $\mathcal{E} = \mathcal{E}_H$. We use stdGalerkin and GaLS with polynomial orders $k = 1, 2, 3$. The MHM methods use $\ell = 1$ in the global level and local finite elements defined by the stdGalerkin and GaLS discretizations with $k = 1, 2, 3$.

As throughout the whole paper, \mathbf{u}_{Hh} , p_{Hh} and $\boldsymbol{\sigma}_{Hh}$ satisfy (3.12) and (4.11), where $(\boldsymbol{\lambda}_{Hh}, \mathbf{u}^{\text{rm}})$ is the solution of (3.10)-(3.11). In the following, \mathbf{u}_h , \mathbf{w}_h , \mathbf{w}_{Hh} are the displacement solutions obtained by the GaLS, stdGalerkin and MHM methods, respectively, and p_h and $\boldsymbol{\sigma}_h = 2G(\underline{\boldsymbol{\sigma}}(\mathbf{u}_h) - p_h I_2)$ are the pressure and stress solutions obtained from the MHM-GaLS method.

Figure 2 compares the solutions of the four methods for all considered values of ν . They use the same orders $k = 1, 2, 3$ and mesh sizes $h = 2^{k-4.5}$, from top to bottom. The global partition in the MHM methods have size $\mathcal{H} = 2^{-1.5}$. For $k = 1$, the MHM-Ga method loses accuracy when increasing the Poisson's ratio (top-left). In all cases, the MHM-Ga improves the accuracy of the stdGalerkin method for a sufficiently high Poisson's ratio. The MHM-GaLS method does not show a pronounced lack of accuracy in the approximation errors, evidencing its locking-free property. However, the high Poisson's ratio affects more the MHM-GaLS than the GaLS method for all k . As expected, the GaLS and MHM-GaLS improve the accuracy of the stdGalerkin and MHM-Ga methods, respectively, when the Poisson's ratio is close to 1/2.

Figure 3 compares the solutions of the MHM-GaLS and GaLS methods using $\nu = 0.4999$, $\mathcal{H} = 2^{3-k} h$ for the MHM-GaLS, and $k = 1, 2$. Both methods are locking-free, as theory predicts. However, some curves on both methods approach the theoretical $O(h^2)$ convergence very slowly. We verified this is not related to a bad choice of parameter α .

6.2. H -convergence tests. In this section, we show numerical tests to verify the MHM-GaLS method's H -convergence rates, and compare the results with the MHM-Ga method. We use a structured global partition with 32 triangles ($\mathcal{H} = 2^{-1.5}$), and polynomial orders $\ell = 1$ and $k = 1, 2, 3$. We highlight that we study the convergence through a skeleton-based H -refinement, keeping \mathcal{H} fixed. The second-level meshes' sizes are $h = 2^{k-3} H$, corresponding to the minimum allowed for well-posedness (see

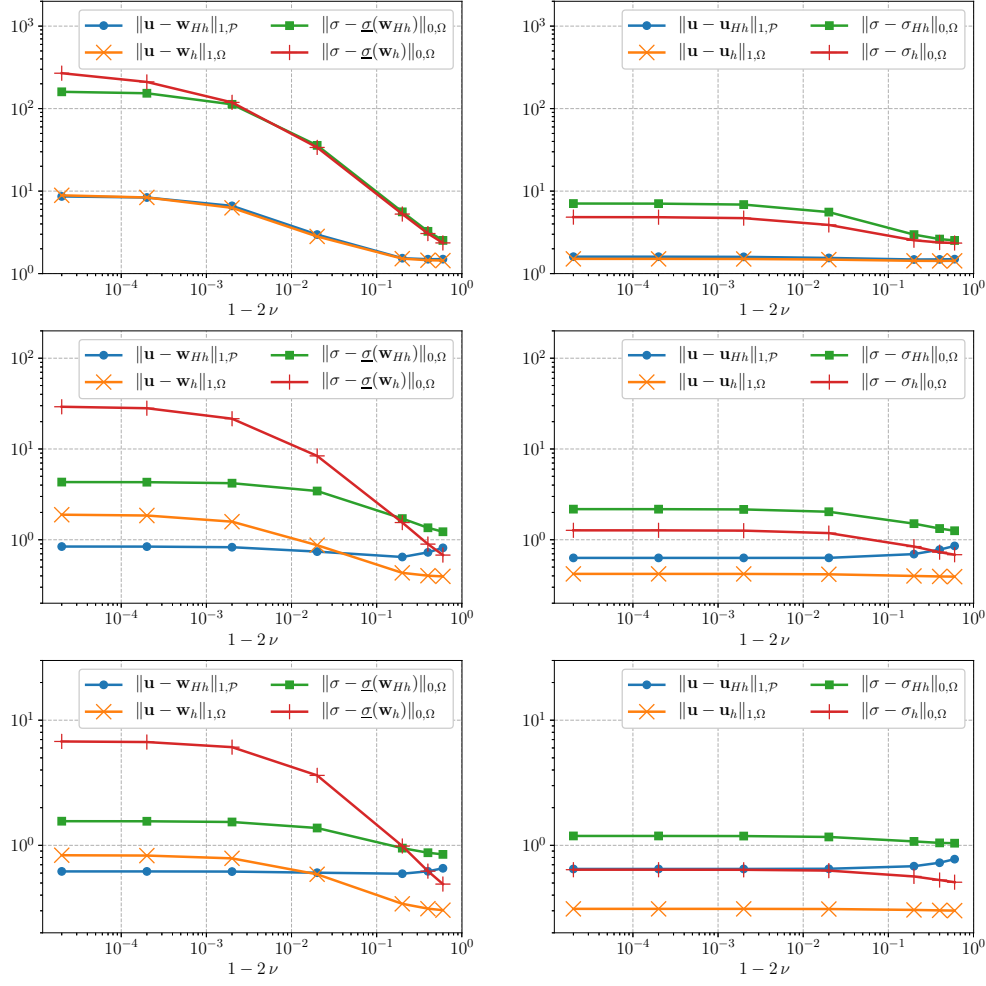


FIG. 2. ϵ -convergence in the four different methods. Orders $k = 1, 2, 3$ and mesh sizes $h = 2^{k-4.5}$, from top to bottom. The global partition's size in the MHM methods is $H = 2^{-1.5}$.

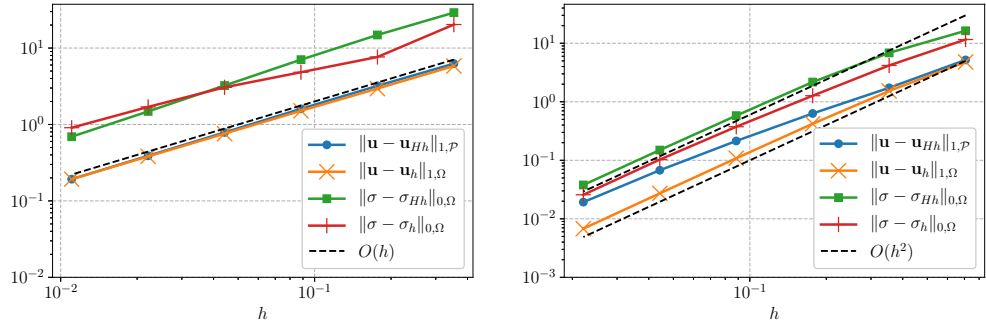


FIG. 3. h -convergence in the MHM-GaLS and GaLS methods using $\nu = 0.4999$, and orders $k = 1$ (left) and 2 (right). The size of the global partition in the MHM-GaLS is $\mathcal{H} = 2^{3-k} h$.

Lemma 4.5). The results use the problem from subsection 6.1 with $\nu = 0.4999$ and $k = 1, 2, 3$.

Tables 1 to 6 show the displacement, stress and pressure errors, and their respective numerical convergence orders. We measure the errors $\mathbf{e}_{Hh} := \mathbf{u} - \mathbf{u}_{Hh}$, $\mathbf{e}_{Hh}^s := \boldsymbol{\sigma} - \boldsymbol{\sigma}_{Hh}$, $e_{Hh}^p := p - p_{Hh}$, $\mathbf{g}_{Hh} := \mathbf{u} - \mathbf{w}_{Hh}$, $\mathbf{g}_{Hh}^s := \boldsymbol{\sigma} - \underline{\boldsymbol{\sigma}}(\mathbf{w}_{Hh})$ using definitions from subsection 6.1. We employed a usual procedure to obtain these orders, namely, we divide the errors in one line by the errors in the line above, and apply the logarithm base 2.

TABLE 1

H-convergence in the MHM-GaLS using $k = 1$. 'ord' is the numerical convergence order.

H	$\ \mathbf{e}_{Hh}\ _{0,\Omega}$	ord	$ \mathbf{e}_{Hh} _{1,\mathcal{P}}$	ord	$\ \mathbf{e}_{Hh}^s\ _{0,\Omega}$	ord	$\ e_{Hh}^p\ _{0,\Omega}$	ord
$\mathcal{H}/2^0$	$5.05 \cdot 10^{-2}$	-	1.58	-	4.77	-	2.74	-
$\mathcal{H}/2^1$	$1.31 \cdot 10^{-2}$	1.94	$7.48 \cdot 10^{-1}$	1.08	1.86	1.36	$9.50 \cdot 10^{-1}$	1.53
$\mathcal{H}/2^2$	$3.22 \cdot 10^{-3}$	2.03	$3.66 \cdot 10^{-1}$	1.03	$8.48 \cdot 10^{-1}$	1.13	$4.07 \cdot 10^{-1}$	1.22
$\mathcal{H}/2^3$	$7.85 \cdot 10^{-4}$	2.04	$1.82 \cdot 10^{-1}$	1.01	$3.83 \cdot 10^{-1}$	1.15	$1.63 \cdot 10^{-1}$	1.32
$\mathcal{H}/2^4$	$1.93 \cdot 10^{-4}$	2.02	$9.05 \cdot 10^{-2}$	1.01	$1.74 \cdot 10^{-1}$	1.14	$6.09 \cdot 10^{-2}$	1.42
$\mathcal{H}/2^5$	$4.78 \cdot 10^{-5}$	2.01	$4.52 \cdot 10^{-2}$	1.00	$8.13 \cdot 10^{-2}$	1.10	$2.21 \cdot 10^{-2}$	1.47

TABLE 2

H-convergence in the MHM-GaLS using $k = 2$. 'ord' is the numerical convergence order.

H	$\ \mathbf{e}_{Hh}\ _{0,\Omega}$	ord	$ \mathbf{e}_{Hh} _{1,\mathcal{P}}$	ord	$\ \mathbf{e}_{Hh}^s\ _{0,\Omega}$	ord	$\ e_{Hh}^p\ _{0,\Omega}$	ord
$\mathcal{H}/2^0$	$2.42 \cdot 10^{-2}$	-	$8.46 \cdot 10^{-1}$	-	1.87	-	$9.31 \cdot 10^{-1}$	-
$\mathcal{H}/2^1$	$2.16 \cdot 10^{-3}$	3.48	$1.71 \cdot 10^{-1}$	2.31	$4.35 \cdot 10^{-1}$	2.10	$2.23 \cdot 10^{-1}$	2.06
$\mathcal{H}/2^2$	$2.23 \cdot 10^{-4}$	3.28	$3.79 \cdot 10^{-2}$	2.17	$1.23 \cdot 10^{-1}$	1.82	$6.80 \cdot 10^{-2}$	1.71
$\mathcal{H}/2^3$	$2.28 \cdot 10^{-5}$	3.29	$8.33 \cdot 10^{-3}$	2.19	$3.52 \cdot 10^{-2}$	1.81	$2.04 \cdot 10^{-2}$	1.74
$\mathcal{H}/2^4$	$2.35 \cdot 10^{-6}$	3.28	$1.86 \cdot 10^{-3}$	2.16	$9.51 \cdot 10^{-3}$	1.89	$5.65 \cdot 10^{-3}$	1.85
$\mathcal{H}/2^5$	$2.54 \cdot 10^{-7}$	3.21	$4.33 \cdot 10^{-4}$	2.11	$2.47 \cdot 10^{-3}$	1.94	$1.48 \cdot 10^{-3}$	1.93

TABLE 3

H-convergence in the MHM-GaLS using $k = 3$. 'ord' is the numerical convergence order.

H	$\ \mathbf{e}_{Hh}\ _{0,\Omega}$	ord	$ \mathbf{e}_{Hh} _{1,\mathcal{P}}$	ord	$\ \mathbf{e}_{Hh}^s\ _{0,\Omega}$	ord	$\ e_{Hh}^p\ _{0,\Omega}$	ord
$\mathcal{H}/2^0$	$2.78 \cdot 10^{-2}$	-	$8.99 \cdot 10^{-1}$	-	1.57	-	$7.09 \cdot 10^{-1}$	-
$\mathcal{H}/2^1$	$2.12 \cdot 10^{-3}$	3.71	$1.41 \cdot 10^{-1}$	2.67	$2.81 \cdot 10^{-1}$	2.48	$1.27 \cdot 10^{-1}$	2.48
$\mathcal{H}/2^2$	$1.93 \cdot 10^{-4}$	3.45	$2.65 \cdot 10^{-2}$	2.42	$5.56 \cdot 10^{-2}$	2.34	$2.54 \cdot 10^{-2}$	2.32
$\mathcal{H}/2^3$	$1.77 \cdot 10^{-5}$	3.45	$4.86 \cdot 10^{-3}$	2.44	$1.03 \cdot 10^{-2}$	2.43	$4.80 \cdot 10^{-3}$	2.40
$\mathcal{H}/2^4$	$1.58 \cdot 10^{-6}$	3.48	$8.70 \cdot 10^{-4}$	2.48	$1.86 \cdot 10^{-3}$	2.48	$8.68 \cdot 10^{-4}$	2.47
$\mathcal{H}/2^5$	$1.40 \cdot 10^{-7}$	3.50	$1.54 \cdot 10^{-4}$	2.50	$3.30 \cdot 10^{-4}$	2.49	$1.55 \cdot 10^{-4}$	2.49

We observe no locking effect on Tables 1 to 3, as the convergence orders stay close to and, in some cases, above the predicted order (see Theorem 5.2). In Tables 1 and 2, we observe higher and lower convergence orders for $\|\mathbf{e}_{Hh}^p\|_{0,\Omega}$, respectively, when compared to the theory. These fluctuations both influence the respective convergence order of $\|\mathbf{e}_{Hh}^s\|_{0,\Omega}$ since $\boldsymbol{\sigma}_{Hh}$ depends on p_{Hh} . An additional $O(H^{0.5})$ convergence appears in Table 3 for all measured errors, which is in accordance with what was found in other MHM methods, e.g., [12].

Tables 4 to 6 shows the MHM-Ga methods' convergence orders that, theoretically [12], should also satisfy the same estimate (5.8). We observe a convergence losses for all orders k . Since the MHM-GaLS method do not present such issues, and they are less

TABLE 4

H-convergence in the MHM-Ga using $k = 1$. ‘ord’ is the numerical convergence order.

H	$\ \mathbf{g}_{Hh}\ _{0,\Omega}$	ord	$\ \mathbf{g}_{Hh}\ _{1,\mathcal{P}}$	ord	$\ \mathbf{g}_{Hh}^s\ _{0,\Omega}$	ord
$\mathcal{H}/2^0$	$8.76 \cdot 10^{-1}$	-	7.29	-	$1.24 \cdot 10^2$	-
$\mathcal{H}/2^1$	$9.90 \cdot 10^{-1}$	-0.18	7.51	-0.04	$2.69 \cdot 10^2$	-1.12
$\mathcal{H}/2^2$	$7.88 \cdot 10^{-1}$	0.33	5.92	0.34	$3.93 \cdot 10^2$	-0.55
$\mathcal{H}/2^3$	$4.45 \cdot 10^{-1}$	0.82	3.48	0.76	$3.98 \cdot 10^2$	-0.02
$\mathcal{H}/2^4$	$1.80 \cdot 10^{-1}$	1.30	1.55	1.17	$2.92 \cdot 10^2$	0.44
$\mathcal{H}/2^5$	$5.69 \cdot 10^{-2}$	1.66	$5.39 \cdot 10^{-1}$	1.52	$1.75 \cdot 10^2$	0.74

TABLE 5

H-convergence in the MHM-Ga using $k = 2$. ‘ord’ is the numerical convergence order.

H	$\ \mathbf{g}_{Hh}\ _{0,\Omega}$	ord	$\ \mathbf{g}_{Hh}\ _{1,\mathcal{P}}$	ord	$\ \mathbf{g}_{Hh}^s\ _{0,\Omega}$	ord
$\mathcal{H}/2^0$	$2.68 \cdot 10^{-2}$	-	$8.63 \cdot 10^{-1}$	-	3.03	-
$\mathcal{H}/2^1$	$2.96 \cdot 10^{-3}$	3.18	$2.55 \cdot 10^{-1}$	1.76	1.24	1.29
$\mathcal{H}/2^2$	$5.22 \cdot 10^{-4}$	2.50	$1.01 \cdot 10^{-1}$	1.33	$9.34 \cdot 10^{-1}$	0.41
$\mathcal{H}/2^3$	$1.16 \cdot 10^{-4}$	2.17	$4.62 \cdot 10^{-2}$	1.13	$8.67 \cdot 10^{-1}$	0.11
$\mathcal{H}/2^4$	$2.58 \cdot 10^{-5}$	2.17	$2.06 \cdot 10^{-2}$	1.16	$7.70 \cdot 10^{-1}$	0.17
$\mathcal{H}/2^5$	$4.73 \cdot 10^{-6}$	2.45	$7.67 \cdot 10^{-3}$	1.43	$5.48 \cdot 10^{-1}$	0.49

TABLE 6

H-convergence in the MHM-Ga using $k = 3$. ‘ord’ is the numerical convergence order.

H	$\ \mathbf{g}_{Hh}\ _{0,\Omega}$	ord	$\ \mathbf{g}_{Hh}\ _{1,\mathcal{P}}$	ord	$\ \mathbf{g}_{Hh}^s\ _{0,\Omega}$	ord
$\mathcal{H}/2^0$	$2.50 \cdot 10^{-2}$	-	$8.06 \cdot 10^{-1}$	-	1.44	-
$\mathcal{H}/2^1$	$1.96 \cdot 10^{-3}$	3.67	$1.33 \cdot 10^{-1}$	2.60	$3.71 \cdot 10^{-1}$	1.95
$\mathcal{H}/2^2$	$2.07 \cdot 10^{-4}$	3.25	$2.73 \cdot 10^{-2}$	2.28	$1.72 \cdot 10^{-1}$	1.11
$\mathcal{H}/2^3$	$2.50 \cdot 10^{-5}$	3.05	$6.37 \cdot 10^{-3}$	2.10	$1.24 \cdot 10^{-1}$	0.47
$\mathcal{H}/2^4$	$2.81 \cdot 10^{-6}$	3.15	$1.39 \cdot 10^{-3}$	2.19	$6.98 \cdot 10^{-2}$	0.83
$\mathcal{H}/2^5$	$2.21 \cdot 10^{-7}$	3.67	$2.21 \cdot 10^{-4}$	2.66	$2.17 \cdot 10^{-2}$	1.69

evident in higher orders ($k = 3$), we conclude the convergence losses for low H are due to the Poisson’s locking. Finally, we shall highlight the MHM-GaLS recovered highly accurate discrete stress fields and, on nearly-incompressible materials, it improves considerably the MHM-Ga’s stress field.

7. Conclusions. We presented a new class of stabilized finite elements, based on augmenting the Galerkin formulation with least squares terms, for the MHM method applied to isotropic elasticity. It allows for the use of heterogeneous shear modulus $G \in W^{1,\infty}(\mathcal{T}_h)$ and Poisson’s ratio $\nu \in L^\infty(\Omega)$. The well definition of the finite elements relies on the choice of positive stabilization parameters α_K , for $K \in \mathcal{P}$, depending only on the polynomial order k , $\text{ess inf}_{\mathbf{x} \in K} G(\mathbf{x})$, and $\|G\|_{W^{1,\infty}(\mathcal{T}_h)}$. We proved the resulting MHM method is Poisson locking-free. The displacement and pressure approximations converge at optimal rates, in their natural norms, to the exact solution, and the rates are independent of ν . Consequently, the stress convergence rate in the L^2 -norm does not depend on ν either. We verify numerically the theoretical convergence rates and locking-free property.

The numerical tests showed that the low-order MHM-Ga method (two-level MHM method with Galerkin finite element) loses precision when the Poisson’s ratio gets closer to $1/2$. Besides that, the MHM-Ga solutions were more accurate on our example than the Galerkin solutions for equivalent mesh sizes. When compared to the MHM-

GaLS method (two-level MHM method with stabilized finite element), we observed an accuracy improvement on all measured errors and, in particular, the stress was significantly better approximated.

Appendix A. Auxiliary results.

We start presenting two lemmas that are auxiliary in the proof of [subsection 4.3](#).

LEMMA A.1. *For every $\mathbf{u}_h \in \tilde{\mathbf{V}}_h(K)$,*

$$(A.1) \quad \sum_{\tau \in \mathcal{T}_h^K} h_\tau^2 \|\nabla \cdot (2G \underline{\boldsymbol{\varepsilon}}(\mathbf{u}_h))\|_{0,\tau}^2 \leq C_I^{-1} \|2G\|_{1,\infty,\mathcal{T}_h^K}^2 \|\underline{\boldsymbol{\varepsilon}}(\mathbf{u}_h)\|_{0,K}^2.$$

Proof. Notice that

$$\begin{aligned} \|\nabla \cdot (2G \underline{\boldsymbol{\varepsilon}}(\mathbf{u}_h))\|_{0,\tau} &= \|\underline{\boldsymbol{\varepsilon}}(\mathbf{u}_h) \nabla(2G) + 2G \nabla \cdot (\underline{\boldsymbol{\varepsilon}}(\mathbf{u}_h))\|_{0,\tau} \\ &\leq \|\underline{\boldsymbol{\varepsilon}}(\mathbf{u}_h)\|_{0,\tau} \|\nabla(2G)\|_{L^\infty(\tau)} + \|2G\|_{L^\infty(\tau)} \|\nabla \cdot (\underline{\boldsymbol{\varepsilon}}(\mathbf{u}_h))\|_{0,\tau} \\ &\leq \|2G\|_{1,\infty,\mathcal{T}_h^K} \left(\frac{1}{h_K^2} \|\underline{\boldsymbol{\varepsilon}}(\mathbf{u}_h)\|_{0,\tau}^2 + \|\nabla \cdot \underline{\boldsymbol{\varepsilon}}(\mathbf{u}_h)\|_{0,\tau}^2 \right)^{\frac{1}{2}}, \end{aligned}$$

where we used [\(4.10\)](#). Then, we can then use [\(4.4\)](#) to obtain

$$\begin{aligned} \sum_{\tau \in \mathcal{T}_h^K} h_\tau^2 \|\nabla \cdot (2G \underline{\boldsymbol{\varepsilon}}(\mathbf{u}_h))\|_{0,\tau}^2 &\leq \|2G\|_{1,\infty,\mathcal{T}_h^K}^2 \sum_{\tau \in \mathcal{T}_h^K} \frac{h_\tau^2}{h_K^2} \|\underline{\boldsymbol{\varepsilon}}(\mathbf{u}_h)\|_{0,\tau}^2 + h_\tau^2 \|\nabla \cdot \underline{\boldsymbol{\varepsilon}}(\mathbf{u}_h)\|_{0,\tau}^2 \\ &\leq C_I^{-1} \|2G\|_{1,\infty,\mathcal{T}_h^K}^2 \|\underline{\boldsymbol{\varepsilon}}(\mathbf{u}_h)\|_{0,K}^2. \quad \square \end{aligned}$$

LEMMA A.2. *There exists $C_{0,K} > 0$ depending only on k, d and $\|2G\|_{1,\infty,\mathcal{T}_h^K}$ such that, for every $(\mathbf{u}_h, p_h) \in \tilde{\mathbf{V}}_h(K) \times Q_h(K)$,*

$$\alpha_K \sum_{\tau \in \mathcal{T}_h^K} h_\tau^2 \|\nabla \cdot (2G \underline{\boldsymbol{\varepsilon}}(\mathbf{u}_h) - p_h I)\|_{0,\tau}^2 \leq 4G_{0,K} \left(\|\underline{\boldsymbol{\varepsilon}}(\mathbf{u}_h)\|_{0,K}^2 + C_{0,K} \|p_h\|_{0,K}^2 \right)$$

Proof. Since

$$\|\nabla \cdot (2G \underline{\boldsymbol{\varepsilon}}(\mathbf{u}_h) - p_h I)\|_{0,\tau}^2 \leq 2(\|\nabla \cdot (2G \underline{\boldsymbol{\varepsilon}}(\mathbf{u}_h))\|_{0,\tau}^2 + \|\nabla p_h\|_{0,\tau}^2),$$

we use [Lemma A.1](#), [\(4.9\)](#), and a classical inverse inequality

$$C \sum_{\tau \in \mathcal{T}_h^K} h_\tau^2 \|\nabla p_h\|_{0,\tau}^2 \leq \|p_h\|_{0,K}^2,$$

(see [\[9, Lemma 1.138\]](#)) to obtain

$$\begin{aligned} \alpha_K \sum_{\tau \in \mathcal{T}_h^K} h_\tau^2 \|\nabla \cdot (2G \underline{\boldsymbol{\varepsilon}}(\mathbf{u}_h) - p_h I)\|_{0,\tau}^2 \\ \leq 4G_{0,K} \left(\|\underline{\boldsymbol{\varepsilon}}(\mathbf{u}_h)\|_{0,K}^2 + C^{-1} \frac{1}{\|2G\|_{1,\infty,\mathcal{T}_h^K}^2} C_I \|p_h\|_{0,K}^2 \right) \end{aligned}$$

Therefore, the proof is complete with $C_{0,K} := C_I / \left(C \|2G\|_{1,\infty,\mathcal{T}_h^K}^2 \right)$. □

The following result is auxiliary in the proof of the stability of B_K .

LEMMA A.3. *There are positive constants C_1 and C_2 such that, for all $p_h \in Q_h(K)$, there exists $\tilde{\mathbf{v}}_h \in \tilde{\mathbf{V}}_h(K)$ satisfying*

$$(A.2) \quad \frac{1}{\|\tilde{\mathbf{v}}_h\|_{1,K}} \int_K p_h (\nabla \cdot \tilde{\mathbf{v}}_h) \, dx \geq C_1 \|p_h\|_{0,K} - C_2 |p_h|_{h,K}.$$

Proof. Given $p_h \in Q_h(K)$, the proof of [10, Lemma 3.3] exhibit a function $\mathbf{v}_h \in \mathbf{V}_h(K) := \{\mathbf{v}_h \in C^0(K) : \mathbf{v}_h|_\tau \in \mathbb{P}_k(\tau)^d, \forall \tau \in \mathcal{T}_h^K\}$ satisfying

$$(A.3) \quad \frac{1}{\|\mathbf{v}_h\|_{1,K}} \int_K p_h (\nabla \cdot \mathbf{v}_h) \, dx \geq C_1 \|p_h\|_{0,K} - C_2 |p_h|_{h,K},$$

where the constants C_1, C_2 do not depend on $p_h \in Q_h(K)$. Since every function $\mathbf{v}_h \in \mathbf{V}_h(K)$ can be written (uniquely) as $\mathbf{v}_h = \tilde{\mathbf{v}}_h + \mathbf{v}^{\text{rm}}$ where $\tilde{\mathbf{v}}_h \in \tilde{\mathbf{V}}_h(K)$, $\underline{\boldsymbol{\varepsilon}}(\mathbf{v}^{\text{rm}}) = 0$ and $\int_K \tilde{\mathbf{v}}_h \cdot \mathbf{v}^{\text{rm}} \, dx = 0$, it holds

$$\begin{aligned} \frac{1}{\|\mathbf{v}_h\|_{1,K}} \int_K p_h (\nabla \cdot \mathbf{v}_h) \, dx &= \frac{1}{\sqrt{\|\mathbf{v}_h\|_{0,K}^2 + \|\nabla \mathbf{v}_h\|_{0,K}^2}} \int_K p_h (\nabla \cdot \mathbf{v}_h) \, dx \\ &\leq \frac{1}{\sqrt{\|\tilde{\mathbf{v}}_h\|_{0,K}^2 + \|\mathbf{v}^{\text{rm}}\|_{0,K}^2 + \|\underline{\boldsymbol{\varepsilon}}(\mathbf{v}_h)\|_{0,K}^2}} \int_K p_h (\nabla \cdot \mathbf{v}_h) \, dx \\ &\leq \frac{1}{\sqrt{\|\tilde{\mathbf{v}}_h\|_{0,K}^2 + \|\underline{\boldsymbol{\varepsilon}}(\tilde{\mathbf{v}}_h)\|_{0,K}^2}} \int_K p_h (\nabla \cdot \tilde{\mathbf{v}}_h) \, dx \\ &\leq \frac{C_{\text{korn},K}}{\|\tilde{\mathbf{v}}_h\|_{1,K}} \int_K p_h (\nabla \cdot \tilde{\mathbf{v}}_h) \, dx, \end{aligned}$$

for all $\mathbf{v}_h \in \mathbf{V}_h(K)$, where we also used Korn's inequality for the space $\tilde{\mathbf{V}}(K)$ from [12]. Thus, we obtain (A.2) by replacing the last expression into (A.3). \square

REFERENCES

- [1] R. ARAYA, C. HARDER, D. PAREDES, AND F. VALENTIN, *Multiscale hybrid-mixed method*, SIAM Journal on Numerical Analysis, 51 (2013), pp. 3505–3531, <https://doi.org/10.1137/120888223>.
- [2] R. ARAYA, C. HARDER, A. H. POZA, AND F. VALENTIN, *Multiscale hybrid-mixed method for the stokes and brinkman equations—the method*, Computer Methods in Applied Mechanics and Engineering, 324 (2017), pp. 29–53, <https://doi.org/10.1016/j.cma.2017.05.027>.
- [3] I. BABUŠKA AND M. SURI, *Locking effects in the finite element approximation of elasticity problems*, Numerische Mathematik, 62 (1992), pp. 439–463, <https://doi.org/10.1007/bf01396238>.
- [4] G. R. BARRENECHEA, F. JAILLET, D. PAREDES, AND F. VALENTIN, *The multiscale hybrid mixed method in general polygonal meshes*, Numerische Mathematik, 145 (2020), pp. 197–237, <https://doi.org/10.1007/s00211-020-01103-5>.
- [5] D. BOFFI, F. BREZZI, AND M. FORTIN, *Mixed Finite Element Methods and Applications*, Springer Berlin Heidelberg, 2013, <https://doi.org/10.1007/978-3-642-36519-5>.
- [6] S. C. BRENNER, *A nonconforming mixed multigrid method for the pure displacement problem in planar linear elasticity*, SIAM Journal on Numerical Analysis, 30 (1993), pp. 116–135, <https://doi.org/10.1137/0730006>.
- [7] DEVLOO, PHILIPPE R. B., FARIAS, AGNALDO M., GOMES, SÔNIA M., PEREIRA, WESLEY, DOS SANTOS, ANTONIO J. B., AND VALENTIN, FRÉDÉRIC, *New $h(\text{div})$ -conforming multiscale hybrid-mixed methods for the elasticity problem on polygonal meshes*, ESAIM: M2AN, 55 (2021), pp. 1005–1037, <https://doi.org/10.1051/m2an/2021013>.

- [8] O. DURÁN, P. R. DEVLOO, S. M. GOMES, AND F. VALENTIN, *A multiscale hybrid method for darcy's problems using mixed finite element local solvers*, Computer Methods in Applied Mechanics and Engineering, 354 (2019), pp. 213–244, <https://doi.org/10.1016/j.cma.2019.05.013>.
- [9] A. EM AND J.-L. GUERMOND, *Theory and Practice of Finite Elements*, vol. 159 of Applied Mathematical Sciences, Springer New York, New York, NY, 1 ed., feb 2004, <https://doi.org/10.1007/978-1-4757-4355-5>.
- [10] L. P. FRANCA AND R. STENBERG, *Error analysis of some galerkin least squares methods for the elasticity equations*, SIAM Journal on Numerical Analysis, 28 (1991), pp. 1680–1697, <https://doi.org/10.1137/0728084>.
- [11] A. T. GOMES, D. PAREDES, W. PEREIRA, R. SOUTO, AND F. VALENTIN, *A multiscale hybrid-mixed method for the elastodynamic model with rough coefficients*, in Proceedings of the XXXVIII Iberian Latin American Congress on Computational Methods in Engineering, ABMEC Brazilian Association of Computational Methods in Engineering, 2017, <https://doi.org/10.20906/cps/cilamce2017-0399>.
- [12] A. T. A. GOMES, W. S. PEREIRA, AND F. VALENTIN, *The MHM Method for Linear Elasticity on Polytopal Meshes*, IMA Journal of Numerical Analysis, 43 (2022), pp. 2265–2298, <https://doi.org/10.1093/imanum/drac041>.
- [13] C. HARDER, A. L. MADUREIRA, AND F. VALENTIN, *A hybrid-mixed method for elasticity*, ESAIM: Mathematical Modelling and Numerical Analysis, 50 (2016), pp. 311–336, <https://doi.org/10.1051/m2an/2015046>.
- [14] C. HARDER, D. PAREDES, AND F. VALENTIN, *On a multiscale hybrid-mixed method for advective-reactive dominated problems with heterogeneous coefficients*, Multiscale Modeling & Simulation, 13 (2015), pp. 491–518, <https://doi.org/10.1137/130938499>.
- [15] C. HARDER AND F. VALENTIN, *Foundations of the MHM method*, in Lecture Notes in Computational Science and Engineering, Springer International Publishing, 2016, pp. 401–433, https://doi.org/10.1007/978-3-319-41640-3_13.
- [16] L. R. HERRMANN, *Elasticity equations for incompressible and nearly incompressible materials by a variational theorem.*, AIAA Journal, 3 (1965), pp. 1896–1900, <https://doi.org/10.2514/3.3277>.
- [17] S. LANTERI, D. PAREDES, C. SCHEID, AND F. VALENTIN, *The multiscale hybrid-mixed method for the maxwell equations in heterogeneous media*, Multiscale Modeling & Simulation, 16 (2018), pp. 1648–1683, <https://doi.org/10.1137/16m110037x>.
- [18] W. PEREIRA AND F. VALENTIN, *A locking-free MHM method for elasticity*, in Proceeding Series of the Brazilian Society of Computational and Applied Mathematics, vol. 5, SBMAC, apr 2017, <https://doi.org/10.5540/03.2017.005.01.0336>.
- [19] D. A. D. PIETRO AND J. DRONIOU, *A hybrid high-order method for leray–lions elliptic equations on general meshes*, Mathematics of Computation, 86 (2016), pp. 2159–2191, <https://doi.org/10.1090/mcom/3180>.
- [20] D. A. D. PIETRO AND A. ERN, *Mathematical Aspects of Discontinuous Galerkin Methods*, Springer Berlin Heidelberg, 2012, <https://doi.org/10.1007/978-3-642-22980-0>.
- [21] P. A. RAVIART AND J. M. THOMAS, *Primal hybrid finite element methods for 2nd order elliptic equations*, Mathematics of Computation, 31 (1977), pp. 391–413, <https://doi.org/10.2307/2006423>.
- [22] L. R. SCOTT AND S. ZHANG, *Finite element interpolation of nonsmooth functions satisfying boundary conditions*, Mathematics of Computation, 54 (1990), pp. 483–483, <https://doi.org/10.1090/s0025-5718-1990-1011446-7>.
- [23] A. VEESER AND R. VERFURTH, *Poincare constants for finite element stars*, IMA Journal of Numerical Analysis, 32 (2011), pp. 30–47, <https://doi.org/10.1093/imanum/drr011>.
- [24] W. ZHENG AND H. QI, *On friedrichs–poincaré-type inequalities*, Journal of Mathematical Analysis and Applications, 304 (2005), pp. 542–551, <https://doi.org/10.1016/j.jmaa.2004.09.066>.